EXPERIMENTAL DETERMINATION OF BETA ATTENUATION IN TOOTH ENAMEL LAYERS AND ITS IMPLICATION IN ESR DATING

EXPERIMENTAL DETERMINATION OF BETA ATTENUATION IN TOOTH ENAMEL LAYERS AND ITS IMPLICATION IN ESR DATING

By

Quan Yang, B.Sc.

A Thesis

Submitted to the School of Graduate Studies

in Partial Fulfilment of the Requirements

for the Degree

Master of Science

McMaster University

MASTER OF SCIENCE (1997) McMASTER UNIVERSITY

(Geology) Hamilton, Ontario

TITLE: Experimental determination of beta attenuation in tooth enamel layers and its implication in ESR dating

AUTHOR: Quan Yang, B.Sc. (Peking University)

SUPERVISORS: Dr. W.J. Rink & Dr. H.P. Schwarcz

NUMBER OF PAGES: XII, 95

ABSTRACT

The principal subject of this thesis is to experimentally determine the beta attenuation patterns in tooth enamel layers, and to examine the predictions of two theoretical models which are involved in the beta dose calculations of ESR dating. One of the models is based on empirical equations (Yokoyama, 1982) and employed by R.Grün (1986) in the DATA software of ESR dating, the other is based on the "one group" transport theory which was incorporated in the ROSY dating programme (B.J. Brennan, et al., 1997).

The theoretical bases of Grün's approximation (i.e. the empirical approach) and the "one group" transport theory are discussed. Their predictions of beta attenuation under 2-π geometry are compared with the results of Monte Carlo simulations, and were then compared with the results of our experimental work, which show clear inclination to the predictions of "one group" theory and Monte Carlo. The previous experiment of Aitken et al.(1985) is also described and its flawed geometric arrangement is discussed.

In this study, two sets of experiments are performed. The first set used pitchblende as the irradiator and employed the configuration of irradiator-absorber-detector, which is aimed to reassess the experiment of Aitken et al. (1985). The second set of our experiments

used a pure beta source of $^{90}Sr(^{90}Y)$ and employed the innovative configuration of tooth enamel pellets in a hole of tooth enamel holder, which substantially solved the problem encountered in the first set (e.g. gamma background subtraction and non-2π geometry, etc.).

Based on our experimental results as well as the discussion of Aitken et al.'s experiment, a conclusion is drawn that the "one group" theory is more reliable in predicting beta doses in ESR dating samples, and consequently, it challenges the ESR ages calculated by DATA software which employs the empirical approach. The comparison of ESR ages calculated by the two dating programmes is shown, and some revisions of published ESR ages based on DATA programme demonstrate the great significance of our experimental results.

ACKNOWLEDGEMENTS

I would like to express my cordial thanks to my supervisors Dr. W.J. Rink and Dr. H.P. Schwarcz for giving me the opportunity of learning and working with them and for their insightful guidance and support of this project. Without their inspiration and supervision, this work can never be done. I also want to gratefully acknowledge Dr. B.J. Brennan for providing some critical data and giving his valuable comments and advisements to this project.

I would like to thank Dr. W.V. Prestwich and Dr. J. Harvey for their very helpful discussions of the experiments. I am also indebted to Jean Johnson, who helped me in several steps of this project, and to Ken McDonald, who provided the modern bovid tooth, which is very precious for our experiments. Thanks to Jim Garrett, who technically helped me throughout the experiments with the tooth enamel pellets. Fred Wicks of the Royal Ontario Museum provided the pitchblende sample.

Specially, I want to thank Dr. H.P. Schwarcz again, who gave me his priceless help when I experienced the hard time of family separation. If this project is considered to be successful, I would give half of the credit to that great improvement of my life. Finally, I must also say a special thank-you to my wife, Xu Zhang, who makes my school days not only a fruitful academic endeavour, but an enjoyable experience as well.

TABLE OF CONTENTS

LIST OF FIGURES

LIST OF TABLES

CHAPTER 1

INTRODUCTION

1.1 Schematic review of geochronologic methods

A very important field of study in geology and archaeology is chronology, namely, to determine the time of geological or archaeological events. Many modern techniques have been utilised in this field of study which brings together physicists, chemists, biologists, geologists, geographers, archaeologists and so on. There are a group of dating methods called "relative age" determination methods, such as those based on geomorphic studies, correlational studies and biological studies; and there are also a lot of methods which provide absolute ages. The majority of these "absolute age" determination methods depend on the laws of radioactivity, such as radiocarbon dating, U-series dating, K-Ar and Ar-Ar dating, cosmogenic nuclide dating, etc., however, there are also several approaches grounded on the accumulated effect of natural irradiation, such as the fission-track method, the luminescence method and most prominently, the electron spin resonance (ESR) method.

It is beyond the scope of this thesis to touch upon any of the other topics listed above, and it is even impossible to cover all the aspects of ESR dating method, which

comprise the theme for this thesis. However, for better comprehension of the work presented, some basic concepts of ESR dating will be introduced.

1.2 Introduction to ESR dating

1.2.1 Basic concepts in ESR dating

The fundamental requirement for any dating methods is to establish the "clock" system, and explain how this "clock" works properly and points to the right time. In the case of ESR dating, such a "clock" can be visualized as an ancient "hourglass" which tells time by the accumulation of sands in the lower pot. Physically, the ESR dating mechanism involves the concepts of ionizing radiation and the formation of trapped electrons (unpaired electrons), where the trapped electrons play the role of those sands dripping into the lower pot of the "hourglass" and are accumulated through time. The concept of "trapped electron" formation in minerals can be explained with the cartoon in Figure 1.1. (Grün, 1989)

Literally, the ESR dating sample is considered to be a kind of insulator which contains two energy levels where electrons might occur, the valence band (ground state) and the conduction band. At the time when the mineral is formed (or recrystallized, or heated), all electrons are at the ground state. With constant exposure to natural irradiation (α-, β-, γ-, and cosmic rays), electrons can be excited from the ground state to the higher energy level (the conduction band). Generally, these excited electrons will recombine with the holes

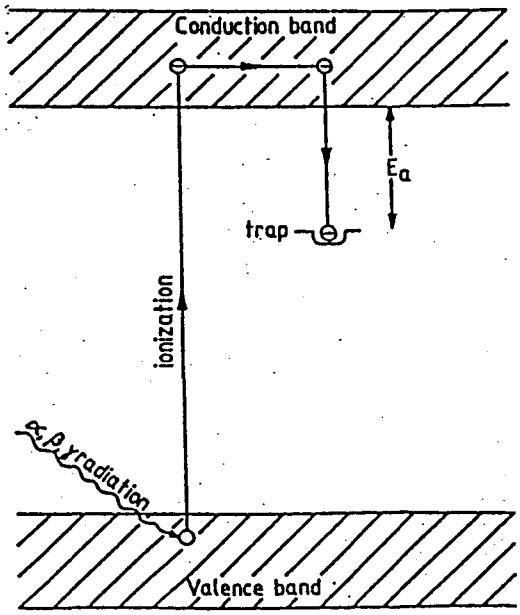

Figure 1.1. Formation of "trapped electrons" in minerals

(positive charged sites) after a short time of diffusion in the conduction band, and quickly emit photons. However, all natural minerals contain certain amount of impurities which form charge deficit sites in the mineral crystal lattices. These crystal defects are capable of trapping a small portion of the excited electrons when they are trying to recombine with the holes in the valence band, thus forming the unpaired electrons (i.e. trapped electrons) which can be detected by the electron spin resonance (ESR) technique, which is a way of observing resonance absorption of microwave power by unpaired electron spins in a magnetic field. The amount of unpaired electrons is known to be proportional to the amount of radiation energy absorbed (based on the fact that each trapped electron possesses a certain amount of energy imparted by ionization irradiation), thus is proportional to the time of irradiation and also the strength of the irradiation. The amount of unpaired electrons is represented by the ESR signal intensity. Therefore, if we can determine the amount of unpaired electrons in a

sample through ESR measurements and also estimate the rate of natural irradiation received by the sample, we can determine the time of its exposure to natural irradiation, which is the ESR age to be determined.

The accumulated effect of ionization irradiation is called "dose", which is defined as the radiation energy absorbed per unit mass, and the rate of such effect is called "dose-rate", i.e. the dose absorbed per unit time, normally, per year. The basic strategy of ESR dating is to measure the accumulated dose AD received by the sample material during the time of its exposure to natural irradiation, and then to determine the time of exposure T after obtaining the dose-rate D(t).

There is an intrinsic relationship among the accumulated dose AD, dose-rate D(t) and the ESR age T:

$$AD = \int_0^T D(t)dt \quad \text{.....(1.1)}$$

where the accumulated dose AD can be determined by the so-called "additive dose method" (refer to Aitken, 1985; Grün, 1989; Ikeya, 1993) and the dose-rate D(t) is generally obtained through the analysis of radioactive elements (uranium, thorium and potassium) in the sample and its surroundings. Complex computations are needed to calculate the α-, β-, γ- and cosmic ray doses, including the estimation of internal and external doses to the sample.

Briefly speaking, ESR dating comprises two major tasks, i.e. to determine the accumulated dose AD, which is implemented by the "additive dose method", and to estimate the dose-rate D(t), which will be briefly discussed in the following part. The ESR age can be obtained through the solution of equation 1.1.

1.2.2 Introduction to the dose rate calculation in ESR dating

The assessment of dose-rate D(t) is one of the critical issues in ESR dating, which has a great influence on the accuracy of ESR dating. There are several approaches to determine the dose rates, such as the use of TLD (thermoluminescence dosimetry) or α- and β- counting, etc., however, the majority of the dose rates in ESR dating are obtained through calculation using the measured values of the radioisotopes (mainly U, Th and K in natural irradiation) in the sample and its surroundings.

To calculate the dose rate, we have to consider the contributions from each radioactive isotope in the decay chains of uranium and thorium, as well as ^{40}K, and for each decay chain, we have to consider separately the α-, β- and γ-doses, which have different characteristics. Water content in the sample and its surroundings can have a strong influence on the dose-rate calculation and is included in the mathematical equations. In some cases, we have to consider the problem of disequilibrium in the radioactive decay chains by measuring some parent/daughter ratios, such as $^{234}U/^{238}U$ and $^{231}Pa/^{235}U$, etc.. Moreover, we have to confront the problem of mobility of some of the radioisotopes, such as the uranium uptake

pattern and the radon loss level. One of the most difficult problems in the dose-rate calculation, however, is the assessment of internal dose and external dose, in which case, the attenuation of different particles (α-, β-, γ-) has to be evaluated.

In the case of homogeneous distribution of radioactive elements with radioactive equilibria in decay chains, the effective sediment dose rate (namely, external dose rate to the sample) $D_\Sigma(SED)$ can be written as: (Grün, 1989)

$$\begin{aligned} D_\Sigma(SED) = {} & C_U\,(k\,G_\alpha\,D_{U\text{-}238\text{-}\alpha}\,W(SED)_\alpha + G_{238\text{-}\beta}\,D_{U\text{-}238\text{-}\beta}\,W(SED)_\beta + G_\gamma\,D_{U\text{-}238\text{-}\gamma}\,W(SED)_\gamma \\ & + k\,G_\alpha\,D_{U\text{-}235\text{-}\alpha}\,W(SED)_\alpha + G_{235\text{-}\beta}\,D_{U\text{-}235\text{-}\beta}\,W(SED)_\beta + G_\gamma\,D_{U\text{-}235\text{-}\gamma}\,W(SED)_\gamma) \\ & + C_{Th}\,(k\,G_\alpha\,D_{U\text{-}232\text{-}\alpha}\,W(SED)_\alpha + G_{232\text{-}\beta}\,D_{U\text{-}232\text{-}\beta}\,W(SED)_\beta + G_\gamma\,D_{U\text{-}232\text{-}\gamma}\,W(SED)_\gamma) \\ & + C_K\,(G_{40\text{-}\beta}\,D_{40\text{-}\beta}\,W(SED)_\beta + G_\gamma\,D_{40\text{-}\gamma}\,W(SED)_\gamma) + C_{Rb}\,(G_{87\text{-}\beta}\,D_{87}\,W(SED)_\beta) \\ & + G_{cos}D_{cos} \qquad \ldots\ldots\ldots\ldots\ldots\ldots\ldots\ldots\ldots\ldots\ldots\ldots (1.2) \end{aligned}$$

and the effective internal dose rate $D_\Sigma(I)$ is given by:

$$\begin{aligned} D_\Sigma(I) = {} & C_U\,(k\,S_\alpha\,D_{U\text{-}238\text{-}\alpha}\,W(I)_\alpha + S_{238\text{-}\beta}\,D_{U\text{-}238\text{-}\beta}\,W(I)_\beta + S_\gamma\,D_{U\text{-}238\text{-}\gamma}\,W(I)_\gamma + k\,S_\alpha\,D_{U\text{-}235\text{-}\alpha}\,W(I)_\alpha \\ & + S_{235\text{-}\beta}\,D_{U\text{-}235\text{-}\beta}\,W(I)_\beta + S_\gamma\,D_{U\text{-}235\text{-}\gamma}\,W(I)_\gamma) + C_{Th}\,(k\,S_\alpha\,D_{U\text{-}232\text{-}\alpha}\,W(I)_\alpha + S_{232\text{-}\beta}\,D_{U\text{-}232\text{-}\beta} \\ & W(I)_\beta + S_\gamma\,D_{U\text{-}232\text{-}\gamma}\,W(I)_\gamma) + C_K\,(S_{40\text{-}\beta}\,D_{40\text{-}\beta}\,W(I)_\beta + S_\gamma\,D_{40\text{-}\gamma}\,W(I)_\gamma) \quad \ldots\ldots\ldots\ldots (1.3) \end{aligned}$$

where:

$D_{\Sigma X}$ = effective dose rate (including attenuation factors, etc.);

$C_{U,\,Th,\,K,\,Rb}$ = concentrations of uranium, thorium, potassium and rubidium

$D_{U\text{-}238}$ = dose rate of the ^{238}U decay chain; (α-, β-, γ- doses are indicated)

$D_{U\text{-}235}$ = dose rate of the ^{235}U decay chain; (α-, β-, γ- doses are indicated)

$D_{Th\text{-}232}$ = dose rate of the ^{232}Th-decay chain; (α-, β-, γ- doses are indicated)

D_{40} = dose rate of ^{40}K-decay; D_{87} = dose rate of ^{87}Rb-decay;

D_{cos} = cosmic ray dose; $W_{\alpha,\beta,\gamma}$ = water correction parameter;

k = alpha efficiency value; $G_{\alpha,\beta,\gamma}$ = attenuation factors;

$S_{\alpha,\beta,\gamma}$ = self-absorption factors;

The water correction parameters $W_{\alpha,\beta,\gamma}$ are derived from the equation:

$$W_{\alpha,\beta,\gamma}=[1+H_{\alpha,\beta,\gamma}(X/(100-X)]^{-1} \quad \text{.....(1.4)}$$

where H_α = 1.49; H_β = 1.25; H_γ = 1.14 and X = water content in wt.%.

The dose rate values (α-, β-, γ-) required in the equations discussed above (i.e. $D_{U\text{-}238\text{-}\alpha,\beta,\gamma}$, $D_{U\text{-}235\text{-}\alpha,\beta,\gamma}$, etc.) are listed in Table 1.1. (after Nambi and Aitken, 1986)

Table 1.1 Released dose rates per ppm U (^{238}U:^{235}U = 138:1) and Th, 1% K and 100 ppm Rb

Decays	Dose rates (μGy/year)		
	Alpha	Beta	Gamma
^{238}U-^{206}Pb	2658	143	112
^{234}U-^{206}Pb	2398	88	110
^{230}Th-^{206}Pb	2103	87	110
^{226}Ra-^{206}Pb	1814	86	110
^{222}Rn-^{206}Pb	1517	86	109
^{235}U-^{207}Pb	124	4.1	1.9
^{231}Pa-^{207}Pb	109	3.5	1.3
$D_{U\text{-}238} + D_{U\text{-}235}$	2781	147	114
^{232}Th-^{208}Pb	738	28.6	52.1
^{40}K		814	242
^{87}Rb		46.8	

Note: Decay chains are assumed to be in secular equilibrium.

Practically, the decay chains are not always in equilibrium, but the difference made by the radioactive disequilibria can be solved by applying the laws of radioactivity and using the intrinsic relationship within the decay chains to calculate the dose rate under radioactive disequilibrium, with some parent/daughter ratios. (Certain simplifying assumptions are needed.) The problems related to the uranium uptake models and radon loss levels can also be treated by making certain adjustments to the dose rate equations. (refer to Aitken 1985 or Grün 1989 for details.)

1.3 Determination of beta Attenuation in ESR dating samples

In the dose rate equations (formulae 1.2 and 1.3), there are two groups of very important parameters, which are the attenuation factors $G_{\alpha,\beta,\gamma}$, and the self-absorption factors $S_{\alpha,\beta,\gamma}$, given by $S_{\alpha,\beta,\gamma} = 1 - G_{\alpha,\beta,\gamma}$. These two related parameters play critical roles in the dose rate calculations, seeing that they are all multipliers in the equations. As will be discussed later (see chapter 2), these two parameters are geometry dependent. Generally, the alpha dose attenuation factor is less important because it can be eliminated (i.e. set equal to zero) by removing about 100 μm of the sample surface. The gamma and cosmic ray attenuation is also less sensitive, considering their much longer range relative to sample dimensions. However, the beta attenuation factor G_β is very important and can never be avoided if the sample dimensions are in the range of several millimeters, which is exactly the range of beta particles. Typically, the beta dose rate (including external and internal) contributes more than 30% of the total dose rate to the sample, thus the accuracy of the beta

dose attenuation factor G_β is very sensitive in the dose rate estimation, and influences the accuracy of ESR age determination.

Essentially, the determination of beta attenuation factor G_β is a problem of determining beta attenuation patterns for different beta sources in different media, which belongs to the scope of beta dosimetry. Monte Carlo simulation is currently the best way of solving this kind of problem, however, the data processing is tedious, and no general solutions or mathematical equations can be achieved through this methodology, which are desired in the age calculation of ESR dating. In order to calculate the beta doses, two analytical approaches are currently employed by ESR dating. One is based on some empirical equations (Yokoyama, et al. 1982 and Grün 1986) and the other is based on the so-called "one-group" transport theory (Brennan et al., 1997). These two theories and their relevant equations were incorporated into computer programmes and involved in determining the ESR ages. The former was employed by DATA programme, (R.Grün, Australian National University, Canberra, Australia) and the latter was used in the ROSY programme. (B.J. Brennan, University of Auckland, Auckland, New Zealand)

The predictions of beta attenuation based on "one group" transport theory have much better agreement with those based on Monte Carlo simulation (Brennan, et al., 1997). However, the empirical equations appeared much earlier (Yokoyama et al., 1982), and most importantly, they were supported by some experimental results (Aitken et al., 1985). Although some scientists have questioned this inconsistency, the problem remained

unsolved, and in practice, most ESR dating researchers have relied on the empirical calculations, i.e. the DATA computer programme, to compute their ESR ages, until the paper published by Rink et al. (1996), which points out that the ESR ages based on the "one group" theory to assess the beta doses have better agreement with the Carbon-14 ages.

The different models of beta attenuation employed by DATA and ROSY programmes can lead to large differences in the age calculations for the same sample. In some extreme cases, the difference can be 30% or even higher. Generally, the ESR ages obtained by DATA calculation are about 5-30% younger than those calculated by ROSY programme, depending on individual situations. Such discrepancy is prominent, and it was apparent that more theoretical consideration and experimental research were needed to clarify this discrepancy. This became the main theme of my Master's research project entitled: **"Experimental determination of beta attenuation in tooth enamel layers and its implication in ESR dating."**

CHAPTER 2

THEORETICAL PREDICTIONS OF BETA ATTENUATION UNDER 2-π GEOMETRY

The assessment of the beta attenuation factor G_β is a problem related to beta irradiation and beta attenuation in continuous media. In this chapter, two theoretical approaches will be discussed, which are employed to estimate this factor in ESR dating, one of which is the empirical approach and the other is based on the "one group" transport theory.

2.1 Basic physics of beta irradiation and beta attenuation

Beta irradiation refers to the exposure of substances to beta particles, which are negatively charged "negatrons" and positively charged "positrons" emitted by atomic nucleus during radioactive decays. Conventionally, a beta particle is considered to be the same as an electron.

The beta particle or electron is a light charged particle which has only about 1/7300 the mass of an alpha-particle (helium nucleus, the heaviest natural decaying particle). It is a very important member in the family of ionizing particles, however, the interaction of beta

particles with medium is quite different from other charged particles (such as alpha particles and various ions) due to their small masses. The passage of beta particles is easily deviated by interacting with the medium's atomic electrons and the interaction of electrons with the Coulomb field of the medium's nuclei causes emission of electromagnetic radiation (bremsstrahlung). Generally, the interaction of electrons with the medium can be visualized as a process of random scattering (both elastic and inelastic), through which the energy of the electrons is lost gradually. The macroscopic manifestation of this process is referred to as beta attenuation.

The beta particles emitted by beta-decays of radioactive elements are characterized by a distribution of energies called a beta-ray spectrum. Characteristically, the energy spectrum of beta particles is a continuous distribution, from zero to a maximum value (E_{max}) equal to the nuclear energy change in the nuclear transition. As an ordinary example, Figure 2.1 (Cross, et al., 1983) displays the energy spectra of beta particles emitted by a $^{90}Sr(^{90}Y)$ beta-source, which will be employed as one of our irradiators in the study of beta attenuation in tooth enamel layers. Note that the fraction of beta-particles emitted near the maximum energy (E_{max}) is very small. A much larger fraction is emitted with the average energy (E_{ave}), which is approximately 1/3 of E_{max}. The range of beta-particles depends on the value of E_{max}, but in calculating the actual radiation dose from a beta-emitter, the E_{ave} value is often used. Noticeably, the spectral shapes sometimes have significant influence in the shapes of dose-depth distributions.

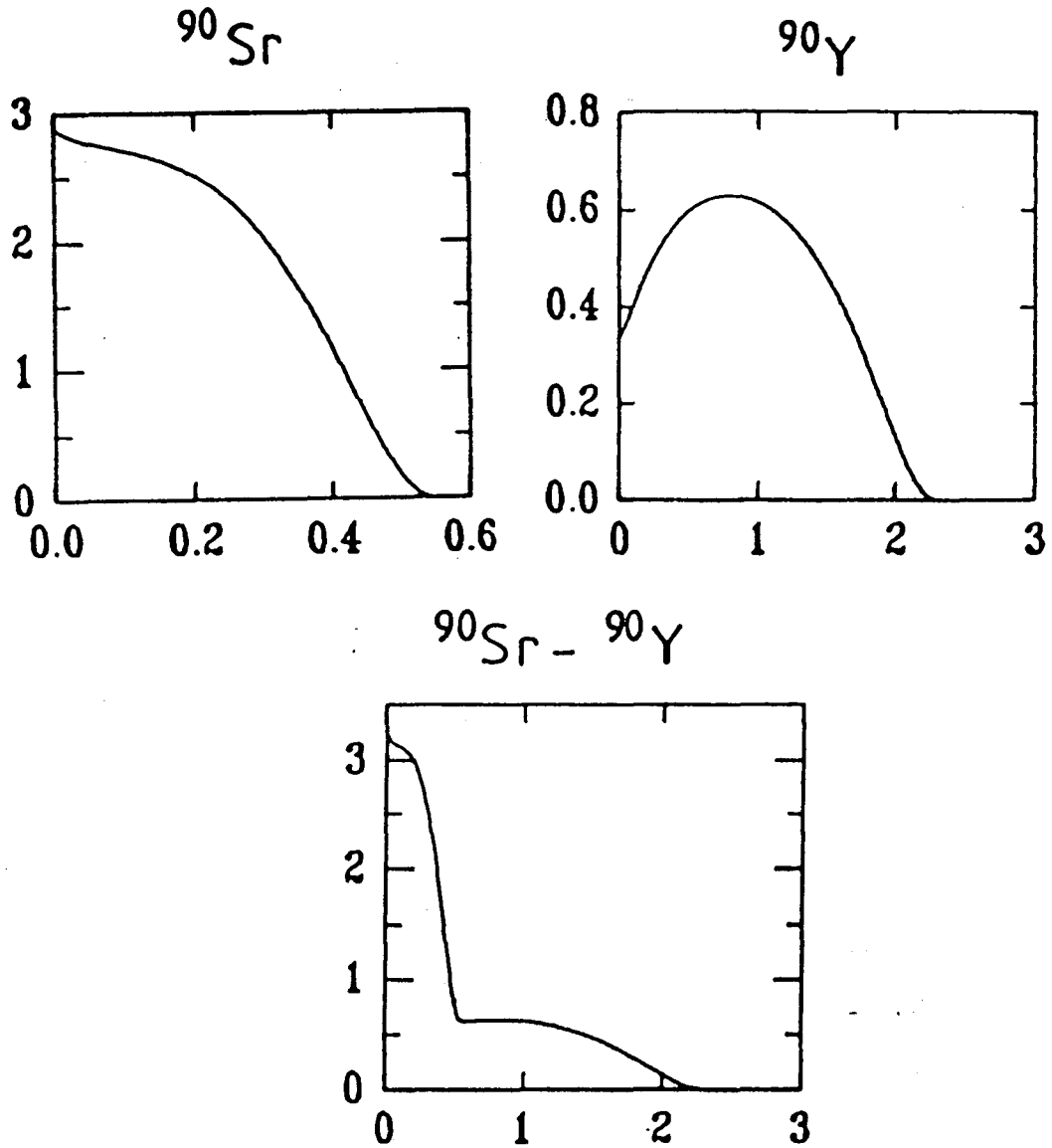

Figure 2.1. Beta-ray spectra of $^{90}Sr(^{90}Y)$ source. ^{90}Y is the daughter of ^{90}Sr. The actual spectrum of a $^{90}Sr(^{90}Y)$ source is the combination of the two individual spectra, which is shown at the lower middle. The horizontal scales give energies in Mev. The vertical scales give the numbers of beta particles per Mev for one transition. (Cross, et al., 1983)

2.2 Beta attenuation under 2-π geometry

The beta attenuation pattern is a collective concept which deals with a large group of electrons when they interact with medium. It depends not only on the energy spectrum of the beta particles but also on the geometry of the source and medium. The simplest geometry of a radioactive source is a "point". The beta attenuation pattern of a point source in medium can be most easily predicted and measured. (Kase, et al., 1990) Another simple geometry is an infinite plane source and infinite medium, which is quoted as 2-π geometry. Strictly speaking, there is no such geometry in nature, but to a first approximation, tooth enamel can be treated as 2-π geometry, although it is usually a hemicylindrical shape, with a finite radius of curvature.

2.2.1 Geometry of the tooth enamel

Tooth enamel is the very hard part of the tooth which is mainly composed of dahllite and carbonate hydroxyapatite (Rink & Schwarcz, 1995). In human tooth, the enamel layer is always outside, surrounding the inner parts, but for large animals (e.g. deer, horse, elephant, etc.), the teeth may have a layered structure which includes enamel, dentine and cementum, as shown in Figure 2.2.

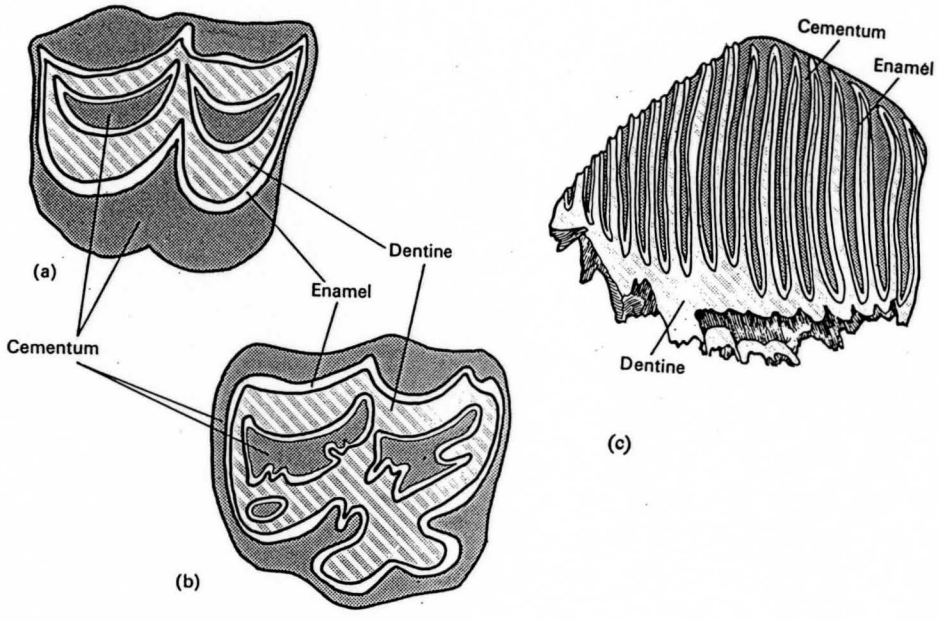

Figure 2.2 Structure of large animal teeth: (a) section of a deer tooth (molar); (b) section of a horse tooth (molar); (c) section of an elephant molar. The enamel layers are sandwiched between layers of dentine and cementum. (Copied from A.E.W. Miles, "Teeth and their origins", Oxford University Press, 1972)

In the form of a fossil tooth, the whole tooth is surrounded by sediment, which is shown in Figure 2.3a. Major components in this view are the sandy sediments and the tooth enamel layers with cementum attached. After the sediments are removed, we can have a clearer view of the tooth structure, as shown in Figure 2.3b. (It's not the same tooth shown in Figure 2.3a, but clearly shows the geometry of an ordinary mammalian tooth.) Notice that the tooth enamel layers form ridges on the chewing surface because of their higher durability than dentine.

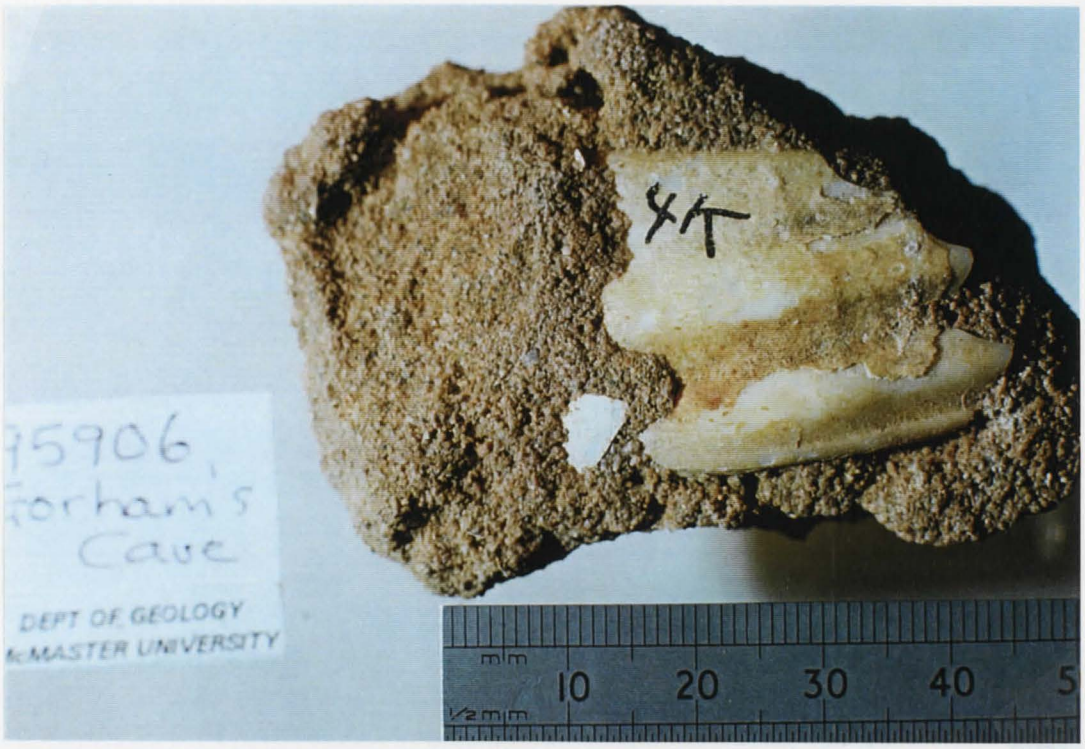

Figure 2.3a Picture of a fossil animal tooth with sandy sediment attached.

Figure 2.3b Picture of a fossil animal tooth with sediments removed.

To simplify the geometry of a real tooth, Figure 2.4 shows the so-called 2-π geometry in the tooth enamel assembly, and will be used as our target for the study of beta attenuation pattern.

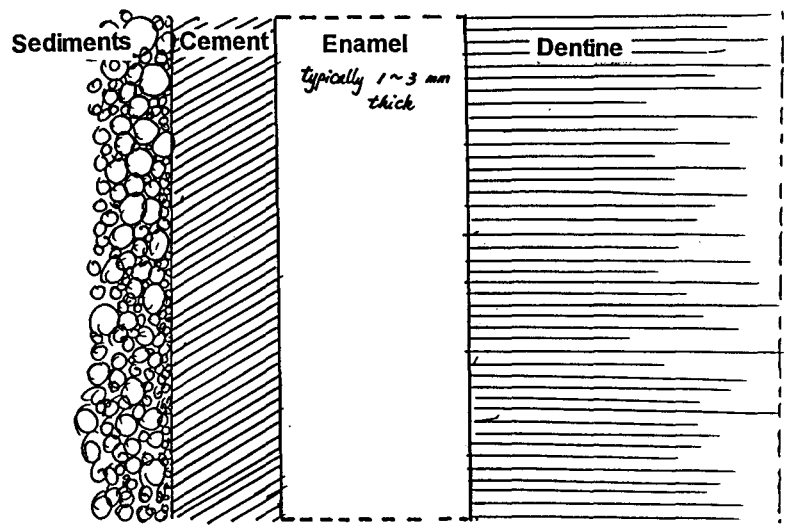

Figure 2.4. Simplified cross section of the layered structure of a tooth

2.2.2 Beta attenuation under 2-π geometry

To determine the beta attenuation pattern, we can consider a one-sided irradiation (2-π geometry) of tooth enamel by dentine or cement (as shown in Figure 2.4). The beta particles emitted by the radioactive elements in dentine and cement will partially penetrate the tooth enamel layer. These energetic particles will lose their energy gradually by interacting with orbital electrons in the medium. The energy loss (attenuation) causes the dose distribution to fall off rapidly in a manner which, in a conventional way (by analogy to the

attenuation of light intensity), can be approximated by an exponential decay of the form:

$$I=I_0 e^{-\mu \cdot d} \quad \text{.....(2.1)}$$

where I_0 is the intensity of the incident beta-ray, and I is the transmitted intensity at depth d, μ is the attenuation coefficient for the absorber (i.e. tooth enamel layer).

Under this approximation (i.e. exponential attenuation), the beta attenuation factor G_β in equations 1.2 & 1.3 can be written as (Yokoyama, 1982):

$$G_\beta=(1-e^{-\mu d})/\mu d \quad \text{.....(2.2)}$$

which is actually an integrated form of equation 2.1, and represents the relative average dose in a layer of depth d, normalized to the half infinite absorber dose.

The beta attenuation factor G_β strongly depends on the value of the attenuation coefficient μ (see equation 2.2), which is the key parameter to be determined by the empirical approach. In the case of "one group" transport theory, however, there is no empirical value of μ involved, and the beta attenuation factor can be obtained by integrating the form of dose-depth variation. Although the beta attenuation factor G_β is important to beta dose calculation in ESR dating, it is convenient for experimental studies and theoretical modelling to study variation of point dose with depth. For simplicity, the term of beta attenuation factor G_β will not be particularly addressed in the following parts, but this value can always be derived from the form of dose-depth variation. (Brennan, et al., 1997)

2.3 Theoretical predictions of beta attenuation under 2-π geometry

2.3.1 Empirical approach

The problem of beta attenuation was initially addressed by experimental physicists, due to the complexities involved in the theoretical prediction of beta particle interactions with various media. Some empirical equations regarding the beta particle behaviour in media were achieved through experiments, which were later developed and modified to deal with the beta attenuation problem.

Physical basis for Grün's approximation

The maximum range of beta particles in a medium is related to their maximum energy, but the relationship is not directly proportional. Flammersfeld (1946) showed that the relationship between the maximum energy E_{max} of a beta spectrum and its maximum range R (in g/cm^2) is given by the following equation:

$$E_{max}=1.92\sqrt{R^2+0.22R} \quad \text{.....(2.3)}$$

where E_{max} is the maximum energy of the beta spectrum, in the unit of Mev. The unit of g/cm^2 is used to describe the range R, because it can be applied to all kinds of materials in spite of their different densities. The range in cm is given by R divided by the density (g/cm^3) of the material.

Based on Flammersfeld's equation, the maximum range of beta-rays can be expressed as an explicit function of their maximum energy:

$$R=0.11\times[(1+22.4E_{max}^{2})^{1/2}-1] \quad \text{.....(2.4)}$$

which is a direct solution from equation 2.3, and this form was first appeared in Yokoyama's paper published in 1982. Worthy of mention is that the maximum range determined is only related to a single beta spectrum. If there are different beta sources emitting different beta spectra, the above equation (equation 2.4) can be applied to deal with them individually, i.e. to determine the maximum ranges of different beta-rays.

Yokoyama (1982) used this equation and obtained the effective range R_{eff} by multiplying 0.75 as: (not well explained in the paper)

$$R_{eff}=0.75R=0.75\times0.11\times[(1+22.4E_{max}^{2})^{1/2}-1] \quad \text{.....(2.5)}$$

and then he gave a relationship (without clarifying its origin) between the effective range R_{eff} and the attenuation coefficient μ in the following equation:

$$\mu=3.3/R_{eff} \quad \text{.....(2.6)}$$

If beta attenuation strictly follows the exponential pattern, the μ value is the only empirical value to determine, because the point dose as a function of depth in the absorber are well determined by:

$$D(d)=D_0 e^{-\mu \times d} \quad \text{.....(2.7)}$$

where D_0 is the point dose at the surface of the absorber, D(d) is the point dose at any depth of the absorber, d is the depth. Notably, there are other forms to express the exponential relationship, such as using the ratio of energy transmitted, and yield a similar equation, which is due to the characteristic of an exponential function.

In reality, the sample is always buried in some kind of matrix which contains radioactive elements, and the surface point dose D_0 of the sample is half of the infinite matrix dose without attenuation (for a one-sided irradiation). The matrix dose D_0 is usually obtained by converting the radioisotope concentrations in the matrix to doses, using a table such as that given by Nambi & Aitken, 1986 (Table 1.1 on page 7). Then, the attenuated point dose in the sample layers is obtained using equation 2.7. Usually, for ESR dating calculations, we care about the average dose D received by a volume of thickness d in the sample, and that can be derived from integration of the point dose equation and then averaging the integrated dose by the thickness, which yields the following: (assuming that the sample is irradiated from one side only, i.e. 2-π geometry) (Aitken et al., 1985; Grün, 1986)

$$D=0.5\times\frac{D_0}{\mu d}\times[1-e^{-\mu d}] \quad \text{.....(2.8)}$$

Moreover, if the sample is treated by removing the surface layer of thickness x to avoid alpha dose, the average beta dose in the remaining sample (total thickness d) can be

calculated by the following equation. (Aitken et al., 1985; Grün, 1986)

$$D_{(d-x)}=[0.5\times\frac{D_0}{\mu(d-x)}]\times[e^{-\mu x}-e^{-\mu d}] \quad \text{.....(2.9)}$$

As implied in the discussion of Flammersfeld's (1946) equation, the μ value determined is specific for an individual beta spectrum, therefore, different beta transitions should correspond to different μ values. If the source contains a decay chain (for example, U-series), the overall beta dose attenuation pattern is a combination of all the individual beta attenuation patterns in the decay chain. In practice, formula 2.4 was applied to all transitions occurring within the decay chain, and formula 2.8 was weighted by the product of the average beta energy and the abundance of this transition, which is proportional to the dose transferred from these electrons to the sample. The sum of the latter can then be plotted in a graph of "average dose" versus "depth" which shows the relative average doses in various depth of samples. Details of this procedure were discussed by Grün (1986), and this model for beta attenuation is incorporated into the programme DATA for β-dose calculation in layers for ESR dating.

Grün's approximation of beta attenuation under 2-π geometry

In order to compare with the experimental results presented later, the dose-depth variation is calculated, following the same procedure to obtain the individual μ values of different beta emitters, as discussed above, but using equation 2.7 for the point dose calculation. The calculations are applied to the uranium series (major beta emitters in U-238 series include ^{234}Th, ^{234}Pa, ^{214}Pb, ^{214}Bi, ^{210}Pb and ^{210}Bi, etc.) and ^{90}Sr source (beta emitters in this source are ^{90}Sr and ^{90}Y) specifically, and the results are shown in Figure 2.5 and Figure 2.6.

Essentially, the Grün's (1986) approximation of the beta dose calculation is based on some empirical equations, which were first reported about half a century ago (Flammersfeld, 1946). There have been more empirical equations developed to describe the "energy-range" relationship of beta particles since that time. (refer to R.D. Evans, 1955) Yokoyama's (1982) contribution was to employ this relationship in the prediction of the "effective range" and then use it to determine the μ value (not well quoted in his paper). The application of Beer's law (i.e. the use of μ values to determine the attenuation pattern) in beta attenuation problem simplifies the model, but it neglects the fact that beta particles are not the same as waves and photons which strictly follow Beer's law. For the beta attenuation problem, a scattering model is considered to be a better approximation, which will be introduced in the following part.

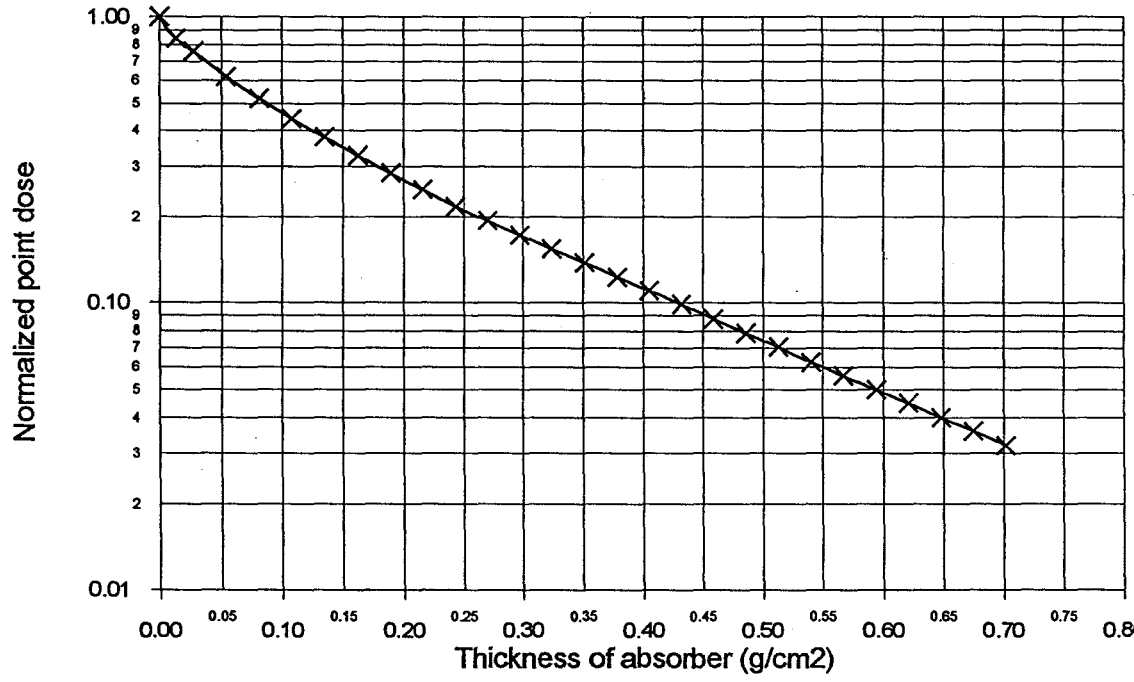

Figure 2.5 Prediction of Dose-depth variation (under 2-π geometry) for U-series (in equilibrium) based on Grün's approximation. (Grün, 1986)

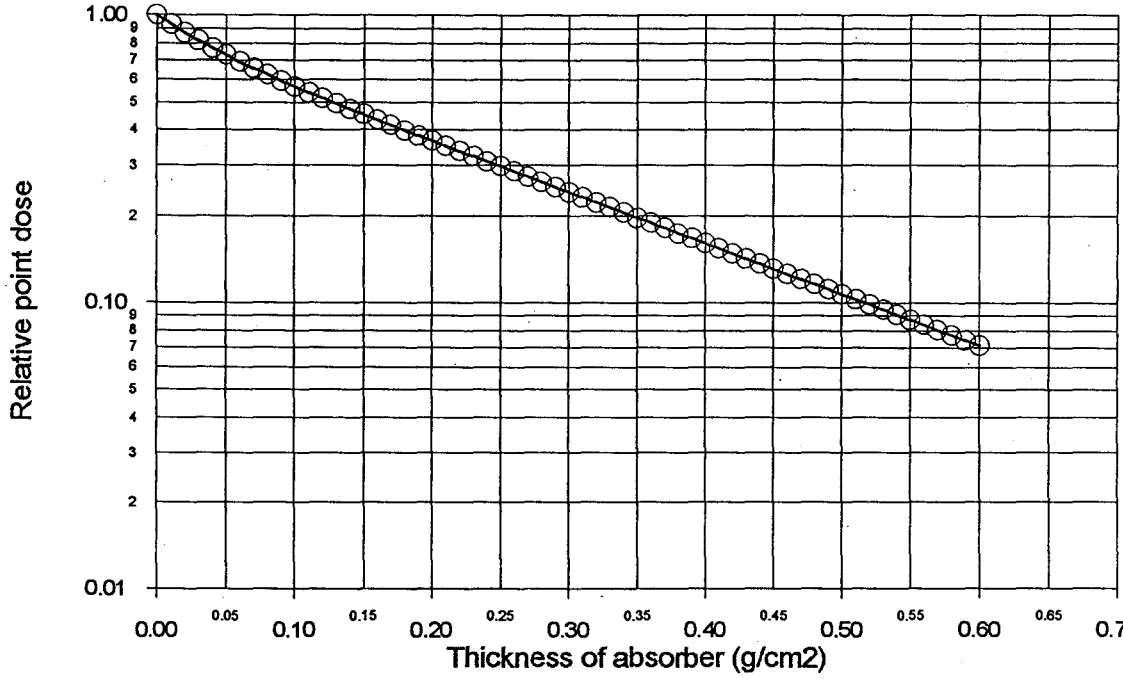

Figure 2.6 Prediction of Dose-depth variation (under 2-π geometry) for $^{90}Sr(^{90}Y)$ source based on Grün's approximation. (Grün, 1986) (Calculated by B.J.Brennan, Physics Department, University of Auckland, New Zealand.)

2.3.2 "One-group" theory approach

The "one group" transport theory was originally developed for modelling neutron transport, but was later proved to be valid in the case of electrons. In 1964, O'Brien et al. first applied this theory to address the beta attenuation problem, and obtained excellent agreement with their experimental results. Further applications of this theory in beta dosimetry and nuclear medicine gave more confidence to its validity. (Prestwich, et al., 1997) It was later employed by the ROSY programme to calculate the beta dose in ESR dating. (Rink et al., 1996; Brennan et al., 1997)

Theoretical analysis

Beta particles at moderate energies are regulated primarily by the processes of elastic and inelastic scattering. The former produces a redirection of energy flow while the latter mainly results in energy absorption. Generally, it is very difficult to describe these processes in an analytical way because of the mathematical complexities involved, however, based on some assumptions, the mathematics can be simplified and some significant results can be achieved through mathematical analysis.

In "one group" transport theory, the basic assumption is to replace the energy spectrum of a given beta emitter by a single group of electrons all at the mean energy (O'Brien, 1964). These monoenergetic electrons are assumed to interact with medium via

a combination of isotropic elastic scattering and complete absorption of part of each beam. The absorption cross section is accepted as the ratio of the stopping power to energy evaluated at the average energy, and the scattering cross section is taken to be the Lewis transport cross section (Lewis, 1950). The geometry involved in the analysis is planar, and boundary conditions are imposed at interfaces to ensure continuity of electron flux in each direction.

Based on the assumptions given above, the dose at different depth D (z) can be expressed as:

$$D(z)=(\frac{\mu_a}{\rho})\times E\times\phi_0(z) \quad \text{.....(2.10)}$$

where z is the one dimensional coordinate, μ_a/ρ is the mass absorption cross section, E is the mean energy of the electrons, and ϕ_0 (z) is the total flux density at depth z.

We assume that the absorption cross section μ_a is the ratio of stopping power to the mean energy E:

$$\mu_a=\frac{S(E)}{E} \quad \text{.....(2.11)}$$

where S(E) is determinable using the Bethe-Heitler expression (W.V. Prestwich, et al., 1997) and E is known. Therefore, the major concern in dose calculation is to determine the total flux density $\phi_0(z)$, because the more particles, the more energy they impart in the medium.

In order to determine the total flux density $\phi_0(z)$ at depth z, we have to start from the basic equations confining the radiation field quantities. Under planar geometry, these quantities depend only upon distance from the reference plane, z, and the direction of propagation, which can be defined by the cosine of the angle with respect to the z-axis, denoted by ω. The general transport equation (Boltzmann equation) is then written as:

$$\omega \cdot \partial\phi/\partial z + (\mu_a + \mu_s)\phi = Y(z, \omega) + \int \mu_s(\omega', \omega) \cdot \phi(z, \omega') \cdot d\omega' \quad \text{.....(2.12)}$$

where $\phi(z, \omega')$ is the angular flux density, $Y(z, \omega)$ is the angular source density, μ_a and μ_s represent the absorption and elastic scattering cross sections respectively.

There is no general solution to the above Boltzmann transport equation, however, under the symmetry given, we know that:

$$\phi(\omega) = \begin{cases} \phi^+ & 0 < \omega < 1 \\ \phi^- & 0 > \omega > -1 \end{cases} \quad \text{.....(2.13)}$$

We also know that $Y(z, \omega)$ and $\mu_s(\omega)$ are actually not ω dependent, but equal one half of their respective totals, with the restrictions of isotropic source and isotropic scattering. The Boltzmann equation finally becomes:

$$\pm\, d\phi^{\pm}/dz + (2\,\mu_a + \mu_s)\,\phi^{\pm}(z) = Y_0(z) + \mu_a\,\phi^{\mp}(z) \quad \text{.....(2.14)}$$

The general solution for this equation is:

$$\Phi^{+}(z) = A\, e^{\nu z} + B\, e^{-\nu z} + G$$

$$\text{and} \quad \phi^{-}(z) = \gamma^{-1} A\, e^{\nu z} + \gamma\, B\, e^{-\nu z} + G \qquad \text{.....(2.15)}$$

where $\nu = 2\sqrt{\mu\mu_a}$, $G = Y_0/2\mu_a$, $\mu = \mu_a + \mu_s$ and

$$\gamma = \frac{\sqrt{\mu} - \sqrt{\mu_a}}{\sqrt{\mu} + \sqrt{\mu_a}}$$

The total flux density is given by:

$$\phi_0(z) = \phi^{+}(z) + \phi^{-}(z) \qquad \text{.....(2.16)}$$

which is needed in the dose equation (formula 2.9).

The parameters A and B in the general solutions of $\Phi^{+}(z)$ and $\phi^{-}(z)$ (equation 2.15) are related to the boundary conditions, and can be determined according to individual situations. If A and B are determined, the total flux density $\phi_0(z)$ is given by equations 2.15 and 2.16, and the dose-depth variation of this group of electrons: D(z), is determined accordingly. (equation 2.9)

"One group" theory's prediction of beta attenuation under 2-π geometry

Based on the "one group" transport theory, a computer code was developed by W.V. Prestwich (McMaster University, Department of Physics, Hamilton, Ontario, Canada) to calculate beta doses in layers of tooth enamel in geometries shown in Figure 2.4. This theory was later incorporated into a full treatment of dose calculation (including α-, β-, γ- and cosmic ray doses) to calculate ESR ages (Brennan et al., 1997).

According to the "one group" theory calculation, the beta doses recorded in the absorber layers (planar geometry) should have a gradient decreasing away from the source, which is displayed by the dose term D(z). Similar to Grün's approximation, the "one group" theory deals with the beta transitions (in the source) one by one, and the total dose gradient D(z) is obtained by applying the transport equations to individual groups of beta particles and then sums the discrete doses to yield the overall dose gradient. So, the beta dose gradient calculated by "one group" theory is also source dependent, which is the same as in the empirical approach.

In the following figures (Figure 2.7 and 2.8), the beta dose gradients of an uranium series source (in equilibrium) and a $^{90}Sr(^{90}Y)$ source are shown, which will later be compared with the experimental results.

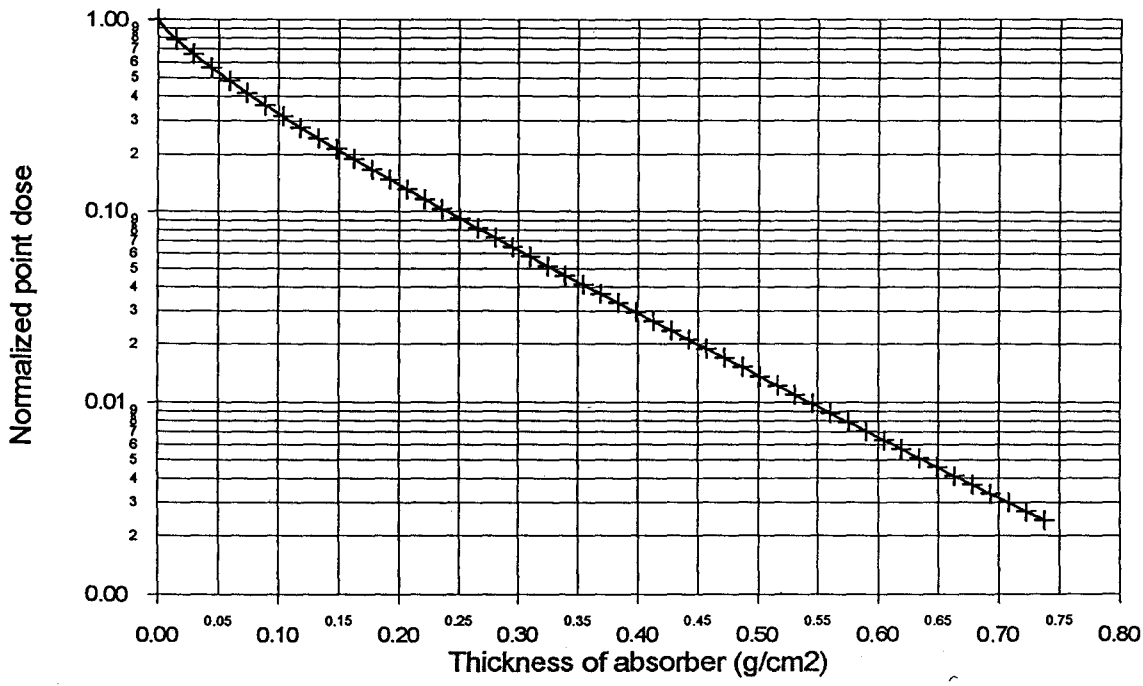

Figure 2.7 Prediction of dose-depth variation (under 2-π geometry) for U-series (in equilibrium) based on "one group" transport theory. (Calculated by B.J. Brennan, Physics Department, University of Auckland, New Zealand.)

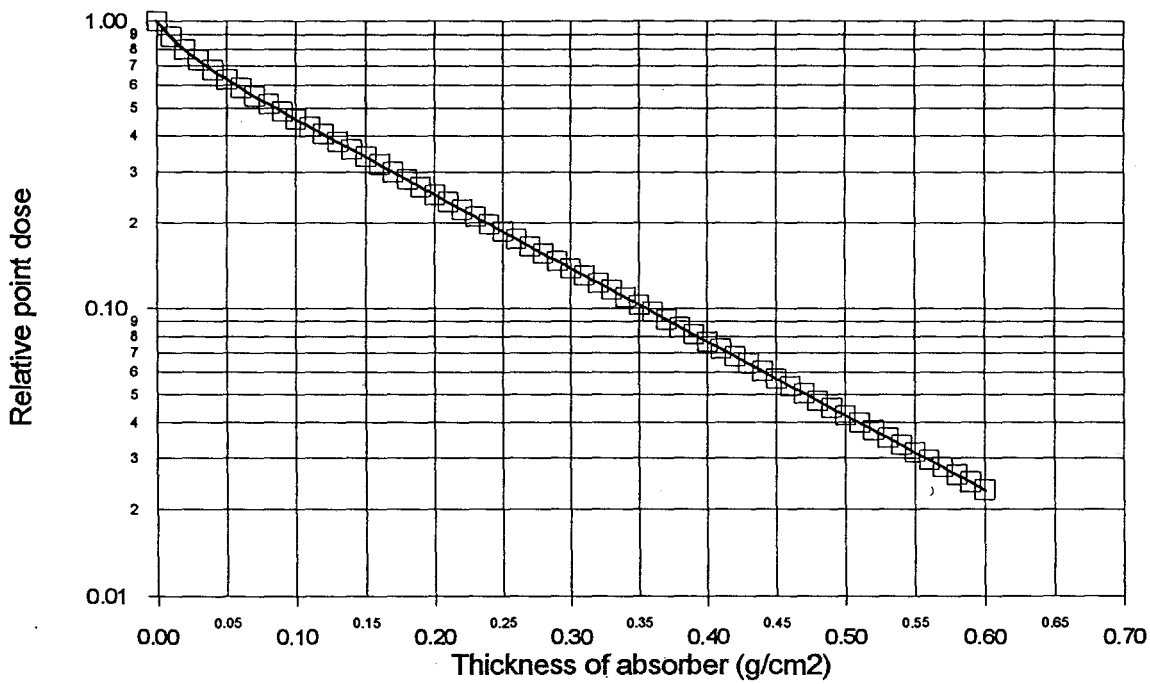

Figure 2.8 Prediction of dose-depth variation (under 2-π geometry) for $^{90}Sr(^{90}Y)$ source based on "one group" transport theory. (Calculated by B.J. Brennan, Physics Department, University of Auckland, New Zealand.)

2.3.3 Monte Carlo approach

Monte Carlo method is a widely used technique to solve problems encountered in mathematics, physics and other sciences, by constructing a random process whose parameters are equal to the required quantities and on which observations can be made by ordinary computational means. From these observations, made on the random process, an estimate is made of the required parameters. In the context of radiation transport, Monte Carlo technique is applied to simulate the random trajectories of individual particles by using machine-generated random numbers to sample from the probability distributions governing the physical processes involved. It is considered to be the best approach in dealing with the dose problems under various conditions.

Generally, a Monte Carlo simulation code has four major components: (1) the cross-section data for all the processes being considered in the simulation, (2) the algorithms used for the particle transport, (3) the methods used to specify the geometry of the problem and to determine the physical quantities of interest, and (4) the analysis of the information obtained during the simulation. Different particle types (e.g., photons, electrons and other charged particles) have different physical processes involved when they are transported through mediums, so, sampling a physical process is the critical part in this technique. In the case of beta particle transportation, all the possible interactions experienced by an electron in the medium have to be taken into account, such as the elastic and inelastic collisions, bremsstrahlung radiation and pair production, etc. Some reference parameters, such as the

cross section data, are input to regulate the interaction, and finally, after a large number of such random processes, the required information can be summarized through the computed results.

It is beyond the scope of this thesis to discuss the Monte Carlo simulation in detail, however, this approach has been proved to be quite accurate in predicting the beta dose distribution under planar geometry. (Kase, et al., 1985) It is therefore very straightforward to think of comparing the beta dose attenuation pattern predicted by Monte Carlo simulation with the results from both DATA and ROSY calculations. Figure 2.9 is the dose-depth variation for uranium series (in equilibrium) obtained through Monte Carlo method.

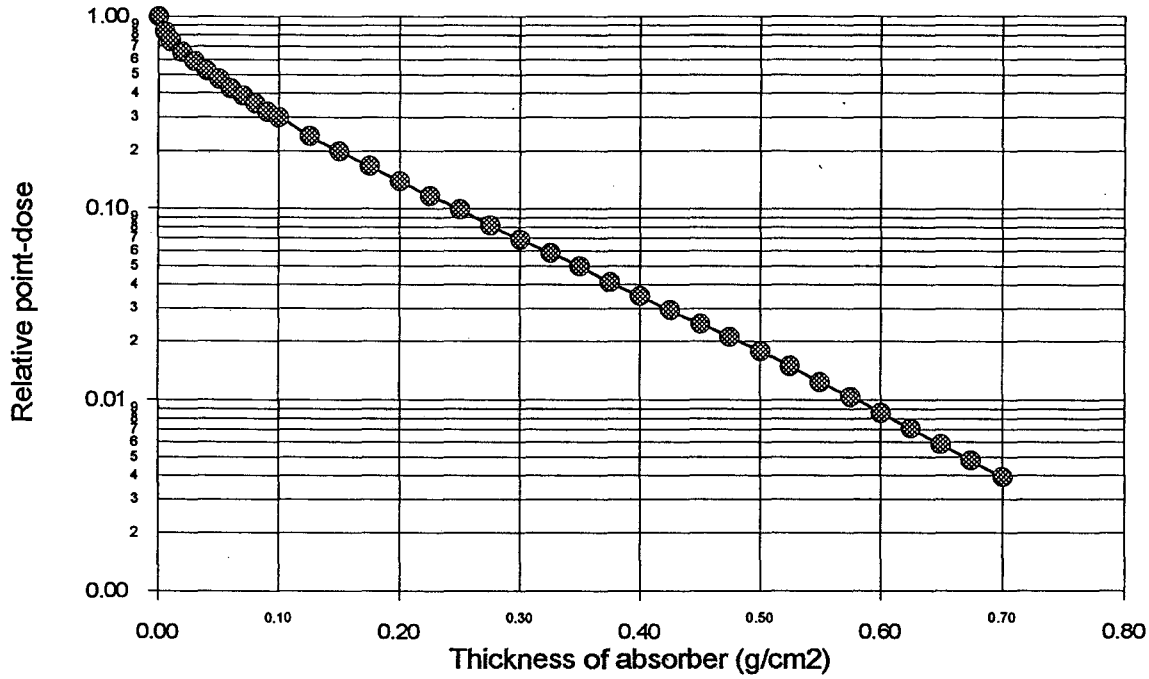

Figure 2.9 Prediction of dose-depth variation (under 2-π geometry) for U-series (in equilibrium) based on Monte Carlo simulation. (Provided by B.J. Brennan, Physics Department, University of Auckland, New Zealand.)

2.4 Comparison of results based on three different theories

Figure 2.10 shows three calculations of "dose-depth variation" for beta attenuation of the U-series (in equilibrium). It is obvious that the result of "one group" theory agrees more closely with the most reliable calculation (Monte Carlo), while the Grün's approximation shows much weaker beta attenuation effect.

Figure 2.11 shows the comparison between "one group" theory's result and Grün's result for the $^{90}Sr(^{90}Y)$ source. Their difference is apparent, showing the same trend as in the case of U-series source, i.e. Grün's prediction of beta attenuation is much weaker than that predicted by the "one group" transport theory. (The Monte Carlo result is not shown in this graph because it was not available at this time, but, by analogy with Figure 2.10, it would also lie much lower than Grün's beta attenuation curve.)

At the present time, the Grün's calculation is well accepted because it is supported by the experimental results of Aitken et al. (1985), and is in wide use due to the wide distribution of the DATA software for calculating ESR ages in tooth enamel and in other layered materials including coral and mollusc shell. However, the discrepancy in the beta dose calculation between Grün's approximation versus "one group" theory and Monte Carlo is problematic, as it casts doubt on the validity of both Aitken's (1985) experiments and Grün's approximation. In fact, ESR ages can be up to 30% lower using "one group" theory relative to those using Grün's approximation (Brennan, et al., 1997). Reassessment of the

previous experiments done by Aitken et al. (1985) and performance of new experiments are essential, because that will help to resolve the problem which beta attenuation model is correct.

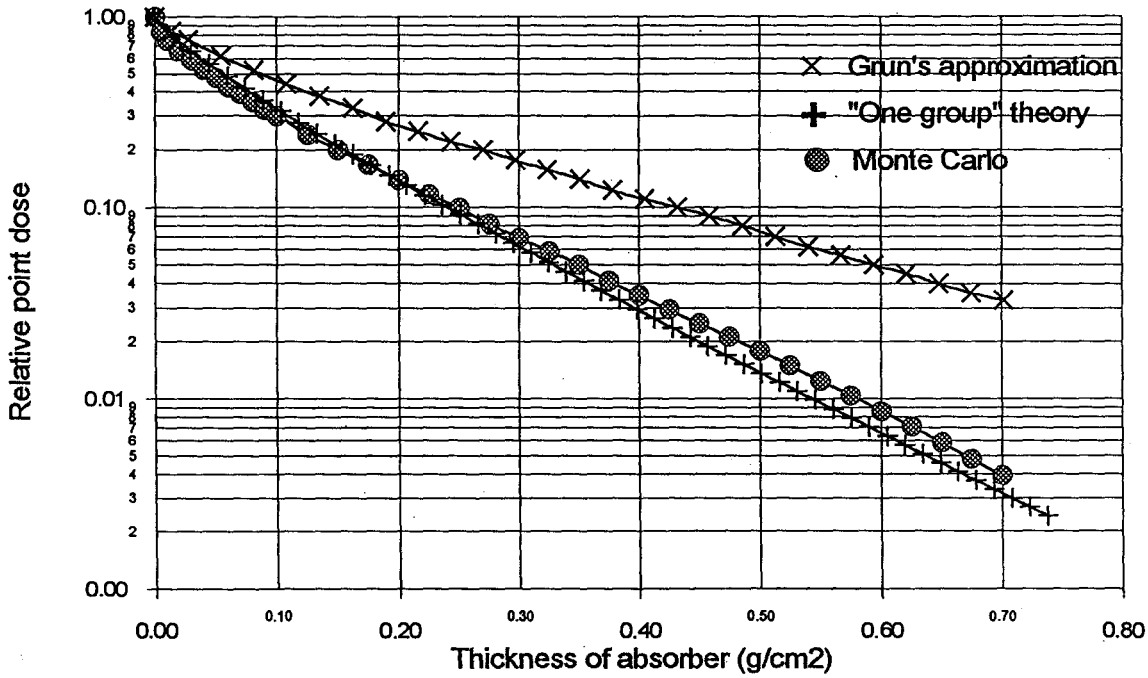

Figure 2.10 Comparison of the theoretical predictions of "dose-depth variation" (under 2-π geometry) for U-series (in equilibrium) by Grün's approximation "X", "one group" theory's calculation "✚" and Monte Carlo simulation "●".

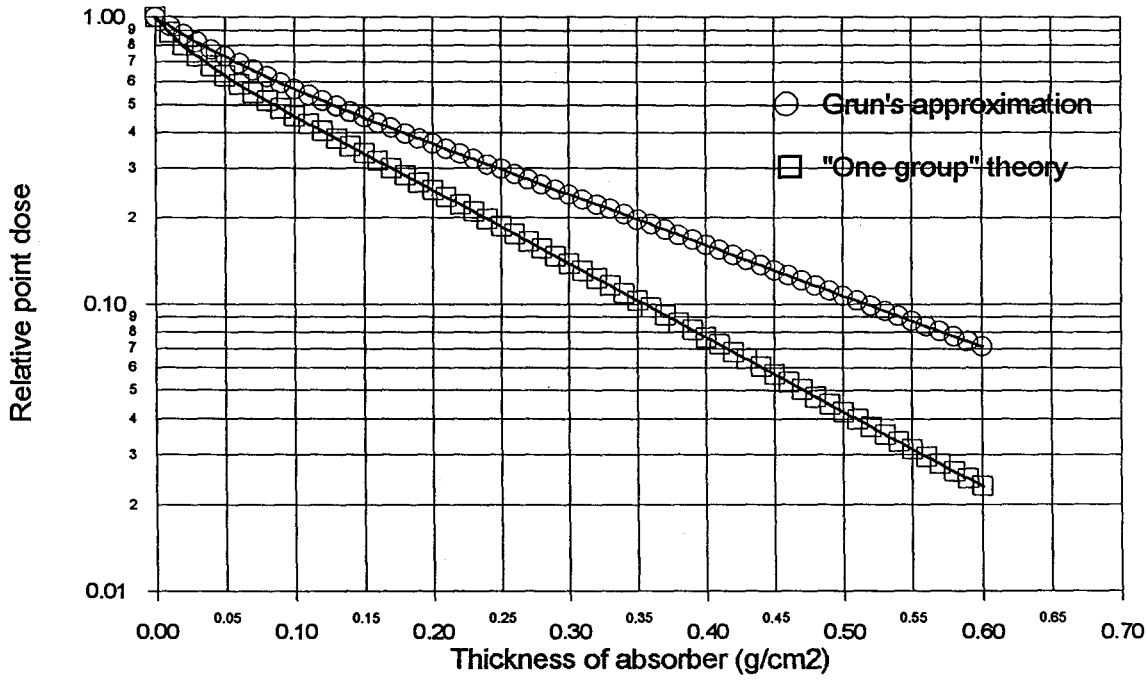

Figure 2.11 Comparison of the theoretical predictions of "dose-depth variation" (under 2-π geometry) for $^{90}Sr(^{90}Y)$ source between Grün's approximation "O" and "one group" theory's calculation "□"

CHAPTER 3

EXPERIMENTAL DETERMINATION OF BETA ATTENUATION IN TOOTH ENAMEL LAYERS

The emphasis of this thesis is actually on the side of experimental work rather than the theoretical analysis. A series of experiments were carried out to determine the beta attenuation effect in tooth enamel layers (and aluminum layers) using both uranium series source (pitchblende) and $^{90}Sr(^{90}Y)$ source. The results using pitchblende as the radioactive source are compared with the results of Aitken et al.'s (1985), which employed exactly the same type of irradiator. In order to strengthen our arguments, experiments using a $^{90}Sr(^{90}Y)$ plate source as the irradiator were also performed, with the innovative experimental configuration of "pellets in a hole", which essentially solved the problem of 2-π geometry.

3.1 Experiments using pitchblende (U-series) as the irradiator

"Pitchblende" is a black, fine-grained rock mainly composed of uraninite, which is a highly radioactive mineral found in hydrothermal sulfide-bearing veins. It is the chief ore of uranium. Commonly, the uranium in pitchblende is at equilibrium with its daughters. It is considered to be a very good radioactive source for the study of uranium series as

applied to ESR or TL dating, because natural sediments are often in radioactive equilibrium.

3.1.1 Aitken et al.'s experiment

In 1985, M.J. Aitken, P.A.Clark, C.F.Gaffney and L. Lovborg published a paper in *Nuclear Tracks* (volume 10, page 647-653) addressing the problem of "Beta and gamma gradient" in ESR dating samples. They presented their experimental and theoretical estimates concerning (1) attenuation within the sample of beta and gamma radiation from the soil, (2) the gamma dose within the sample due to its own radioactivity, and (3) the soil gamma dose in the proximity of boundaries between regions of differing radioactivity. This paper covered a wide range of problems related to beta and gamma dose evaluation, and could be regarded as a cornerstone for the dose rate calculation in ESR dating. One of the significant problems addressed by Aitken et al. is regarding the beta dose attenuation in dating samples. They did a group of experiments to assess the beta dose gradient in planar geometry. One of them employed pitchblende as the irradiator, which was intended to simulate the irradiation by uranium series, and the other used monazite to simulate the thorium series. These two experiments were the same in experimental arrangement.

The basic strategy of the experiments is to measure the doses imparted by beta-rays (unfortunately, gamma-rays are also emitted from pitchblende, but their effects can be removed) after they have penetrated different thicknesses of absorbers. (see Figure 3.1 for their experimental setting) The beta attenuation effect can therefore be determined by

observing that the doses recorded in the detectors decreases with increasing thickness of the absorbers.

In both experiments, TL (thermoluminescence) phosphor was used as the detector, which was composed of natural fluorite. The TL induced in the fluorite was measured using the lamp oven arrangement developed for beta TLD. It is indisputable that the system described in the experiments is a good approach for dose measurement, which will not be discussed further here, however, there might be some minor problems related to the backscattering effect of the copper tray holding the fluorite grains, and effects related to the resin in which the fluorite was embedded. In both experiments, aluminum was used as the material for absorbers.

An important feature of Aitken et al.'s experimental setting is the arrangement of the source, absorber and detector (see Figure 3.1). During the experiment, the source-phosphor distance was kept constant, with increasing thickness of the absorber (maximum thickness of Aluminum absorber is 5 mm). This design is aimed to avoid the influence of gamma background variation which is distance dependent due to the limited dimensions of the planar source. (If the irradiation is under strictly 2-π geometry, i.e. the planar source and planar absorber are infinitely large, there will be no distance dependence for the gamma background.) Unfortunately, this distance which separates the source from the detector leads to the violation of 2-π geometry. (refer to Figure 3.1)

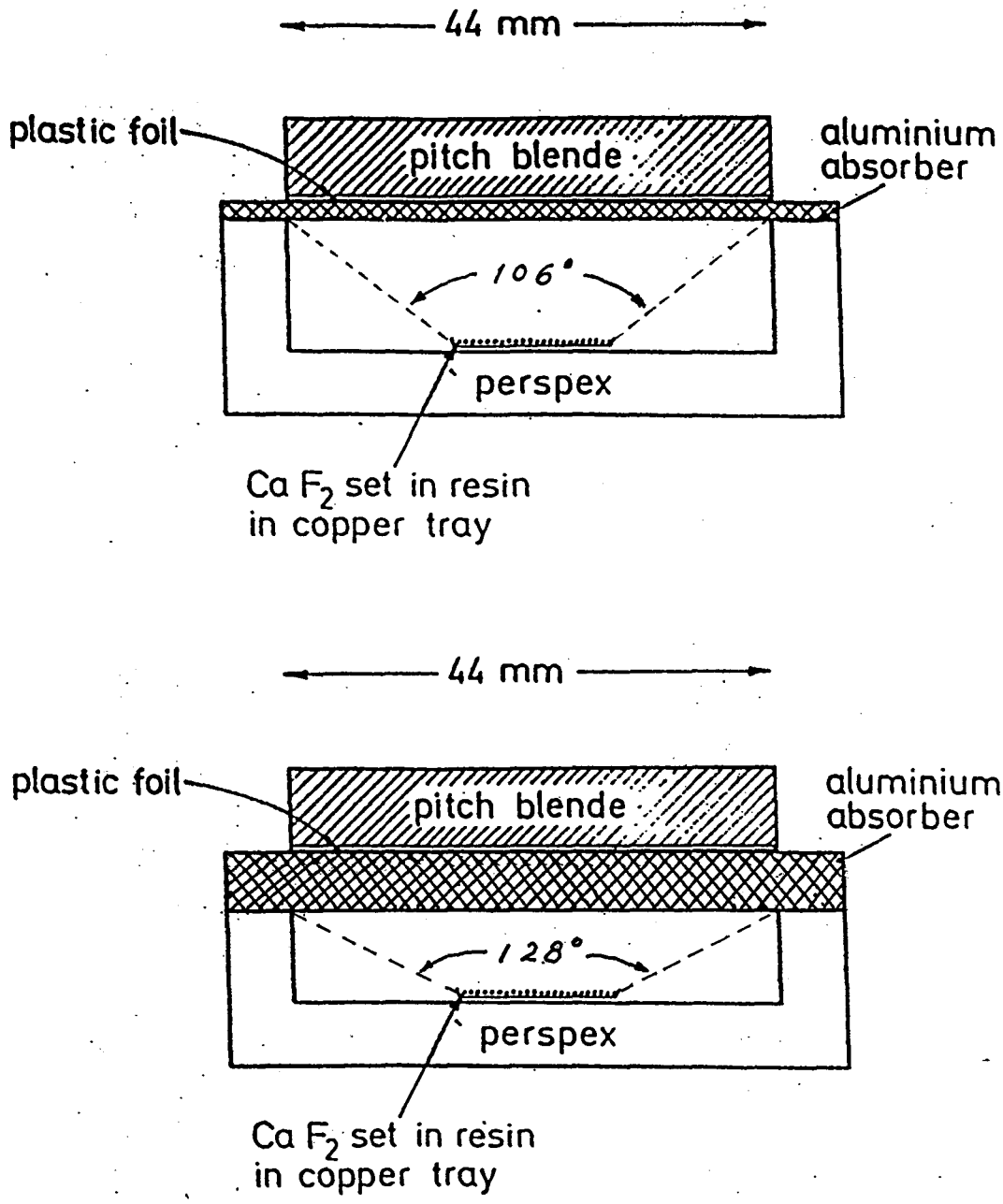

Figure 3.1 Arrangement of Aitken et al.'s(1985) experiments for beta attenuation measurements with pitchblende (U-series) source. The upper and lower settings illustrate the geometries with thinner and thicker absorbers. (lower geometry is the thickest absorber case) The angles indicated are for later discussions. (Copied from Aitken et al. 1985)

Because the uranium series emit both beta and gamma-rays, the subtraction of the gamma background is essential in obtaining the correct attenuation curve of beta rays. Considering the negligible attenuation of gamma rays (within 5mm of aluminum absorber), the gamma contribution is taken to be constant for all absorbers. Moreover, with 5 mm of aluminum absorber, the beta rays are attenuated almost to zero, thus the dose recorded with 5 mm absorber can be treated as pure gamma dose, which was subtracted to remove the effects of gamma doses.

Figure 3.2 (Aitken et al., 1985) shows the result of "relative beta dose versus absorber thickness", which was obtained by subtracting the gamma background from the total dose attenuation curve. (Both the total dose curve and beta dose curve are shown in the graph.)

Figure 3.2 Experimental result (for pitchblende source) of Aitken et al.'s (1985) beta attenuation measurements (using the experimental arrangement shown in Figure 3.1) The dose in this plot is expressed as percentage of the dose recorded for zero thickness of absorber. The straight line (exponential) is the beta attenuation curve after subtracting the gamma background, while the gamma background is considered to be the dose recorded for very thick absorbers (~ 5 mm).

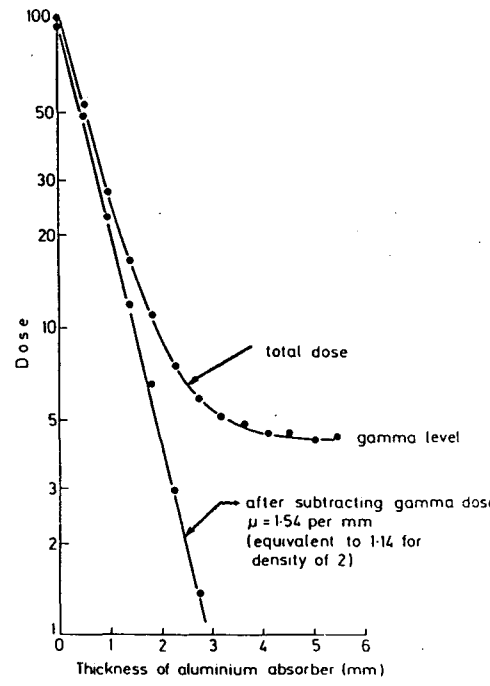

The beta attenuation showed an exponential dependence on thickness (refer to Figure 3.2), with an attenuation coefficient (μ) of 1.54 mm^{-1} (for aluminum absorber). The results were similar for monazite (8.5% Th) except that the μ value was 1.78 mm^{-1} (for aluminum absorber). Since for materials of similar atomic number the attenuation coefficient (μ) is inversely proportional to density (ρ), these results can be converted to tooth enamel absorbers (the density for aluminum is 2.7 g/cm^3, and for tooth enamel is about 2.95 g/cm^3), which are 1.68 mm^{-1} for U-series and 1.94 mm^{-1} for Th-series. Another expression to describe the attenuation property of materials is the "mass attenuation coefficient" (μ/ρ), which is consistent for all materials (for the same type of irradiation). The mass attenuation coefficients (for β-irradiation) obtained by Aitken et al.'s experiments are 5.7 cm^2/g for pitchblende (U-series), and 6.6 cm^2/g for monazite (Th-series).

As discussed in the previous chapter, Aitken et al.'s experiments support DATA's prediction (i.e. Grün's approximation) of beta attenuation style in thin layers, which is demonstrated by the comparison of their result with Grün's approximation in the following plot. (Figure 3.3)

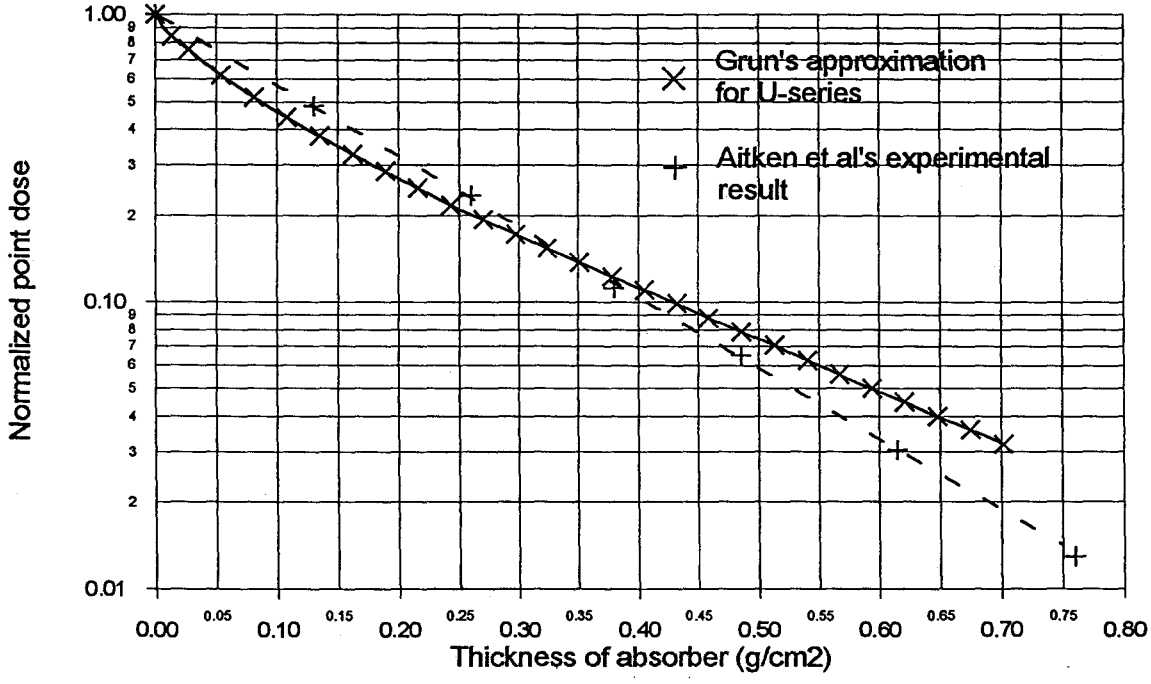

Figure 3.3 Comparison of Aitken et al.'s (1985) experimental result (using pitchblende as the irradiator) with the theoretical prediction of beta attenuation (under 2-π geometry) for U-series (in equilibrium) based on Grün's approximation (Grün, 1986).

3.1.2 Our experiments

Experimental design to reassess Aitken et al.'s work

The basic strategy of our experiment is exactly the same as that in Aitken et al.'s experiment, i.e. using TL phosphor to measure the dose attenuated by different thicknesses of absorbers, however, we used both aluminum and real tooth enamel slabs as the absorbers, because the latter is the substance we wished to determine the beta attenuation effect in.

The pitchblende used in our experiment was originally irregular-shaped, with dimensions of about $1.5 \times 2 \times 3$ cm^3. In order to obtain a flat surface for 2-π geometry irradiation, we cut the nugget into two pieces, both with one shiny surface. One of them was then carefully coated with a very thin layer of epoxy glue (25-50 μm), under strict vacuum condition to avoid any air inclusions. This coating was aimed to prevent radon loss from the pitchblende, and also for the prevention of radioactive contamination of the absorber. After the pitchblende source was well prepared, we had the flat surface radiographed by a professional photographer to see if the radioactivity was evenly distributed. The developed radiograph (negative) proved that our source surface was flat and homogeneous, which was desired in the experiment.

The tooth enamel absorber slabs were prepared from a large mastodon fossil tooth (from Ingleside, Texas, provided by E.L. Lundelius). The enamel layer of this tooth was

> 4 mm in thickness. In order to obtain large plates of tooth enamel (average surface area: 10 × 10 mm^2) of varying thickness, a grinding device was made of copper to facilitate the grinding process (refer to Miles, 1967, page 78). Using this apparatus, we could produce precisely parallel tooth enamel pieces without breaking them, although this was very time-consuming. The aluminum absorbers (round discs of 15mm in diameter) were cut from a pure aluminum rod (with both surfaces polished to ensure their flatness), and those very thin pieces were obtained by rolling. In both processes, a Mitutoyo digimatic gauge (precision ± 2 μm) was employed to measure the thicknesses of the slabs.

The dose detector employed in our experiments was a commercial TLD badge (Panasonic UD804), which was designed for the measurement of environmental gamma dose and beta dose. There are three detecting elements in each TLD, whose doses can be read by a calibrated Panasonic TLD reader. The detecting element is made of $CaSO_4$:Tm grains (100 μm size) attached to a very thin substrate layer of polyamide film (0.011 g/cm^2), in the form of a disk 3 mm in diameter. A photocopy of the TLD (with the sheath removed) we used in our experiments is shown in Figure 3.4, along with our experimental arrangement.

In our experiments, the arrangement was slightly different from Aitken et al.'s (Figure 3.4). The absorber was placed directly on the surface of the pitchblende. The detector was one of the detecting elements of the TLD, with the sheath removed. When the TLD element was positioned on top of the absorber, it was centered to keep at least 3 mm of distance from either edges of the absorber. Due to the fact that there was a 0.011 g/cm^2

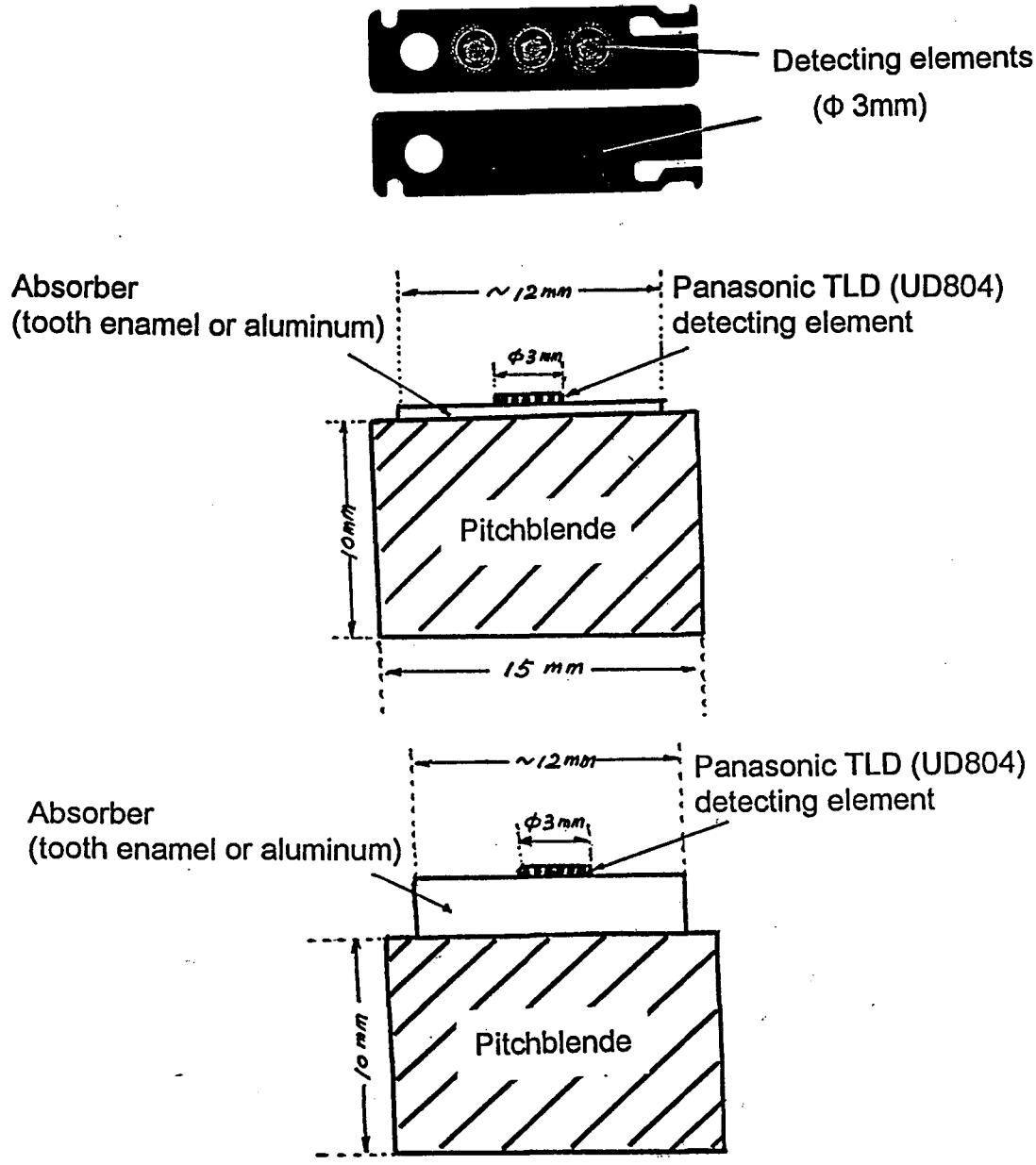

Figure 3.4 Upper (black figures): two-side photocopies of the Panasonic TLD we used. Lower (experimental arrangement): our experimental settings with pitchblende (U-series) source. The upper geometry is the thinner absorber case; the lower geometry is the thickest absorber case. Considering the range of beta particles (~2 mm in tooth enamel), the relationship among the source, absorber and detector can be viewed as effective 2-π geometry. (refer to the text)

thick polyamide substrate to hold the $CaSO_4$:Tm grains, some absorption was expected before the beta rays reached the real dose monitor (i.e. $CaSO_4$:Tm grains), however, it is considered to be minor compared to other possible uncertainties, such as the gamma background subtraction. Fortunately, the backscattering problem was avoided in our experimental setting, which might have affected Aitken et al.'s experiment, because our detector was set into a low-Z thin plastic backing.

Further concerns may be related to the sensitivity of the $CaSO_4$:Tm phosphor used in Panasonic TLD, which is energy dependent. However, the energy dependence of this material is very suitable for the beta dose measurement of natural uranium series, which is illustrated by its "energy dependence" curve in Figure 3.5. (The relative response is obtained by comparing with the calibrated dose.)(Yamashita, et al., 1972)

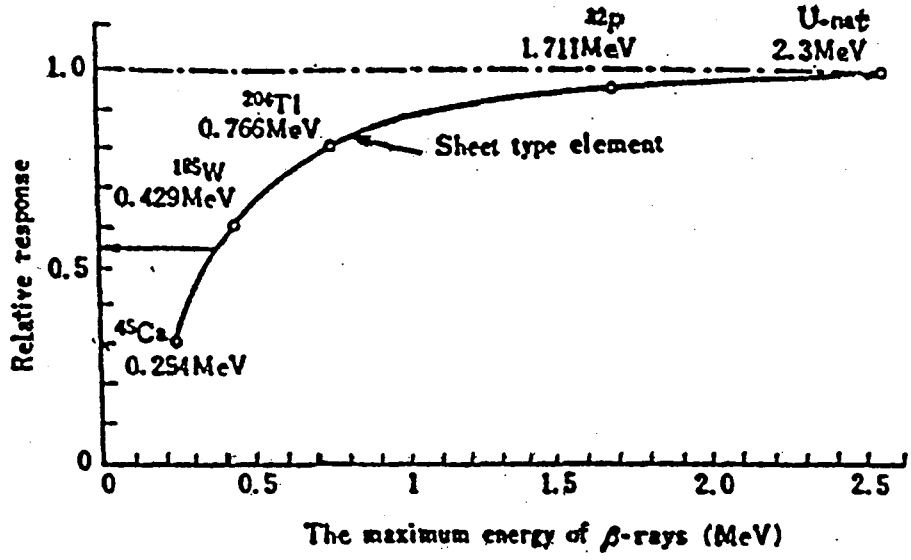

Figure 3.5 Energy response of $CaSO_4$:Tm dosimeters for β-rays.

The "energy dependence" curve (Figure 3.5) shows that there is a plateau (for the sheet type detecting element, as used in the Panasonic UD804) at the energy region of uranium series beta decays. If we assumed that the energy spectra of beta rays didn't alter too much after penetrating a layer of absorber, the problem induced by TLD energy dependence was not so significant, and was therefore ignored in our data processing. There was a similar assumption (unstated) in Aitken et al.'s experiments for their fluorite TL phosphor detectors.

Attenuated doses were measured successively, with different thicknesses of absorbers. (The irradiation time was one day for each measurement, and the delay time between irradiation and measurement was always half an hour.) In order to remove the effects of gamma background, we measured the distance dependent pattern of the irradiation field (in air) by measuring the doses received by the detector with increasing distance between the detector and the surface of the pitchblende irradiator, but without absorbers. This was done by utilizing different thicknesses of strips (thickness was precisely measured), which were obtained by stacking various numbers of thin film strips (1 mm×0.2 mm×200 μm) cut from a sheet of photographic negative film (200 μm in thickness), to support the TLD away from the pitchblende surface. (Practically, two strips of the same thickness were placed on either ends of the source surface to ensure fully exposure of the detecting element to the β- and γ- irradiations from any angle of the pitchblende surface.) A distance dependence curve for the irradiation field was then established. After all the measurements, we built up the "background curve" and the original "attenuated dose curves" as shown in Figure 3.6.

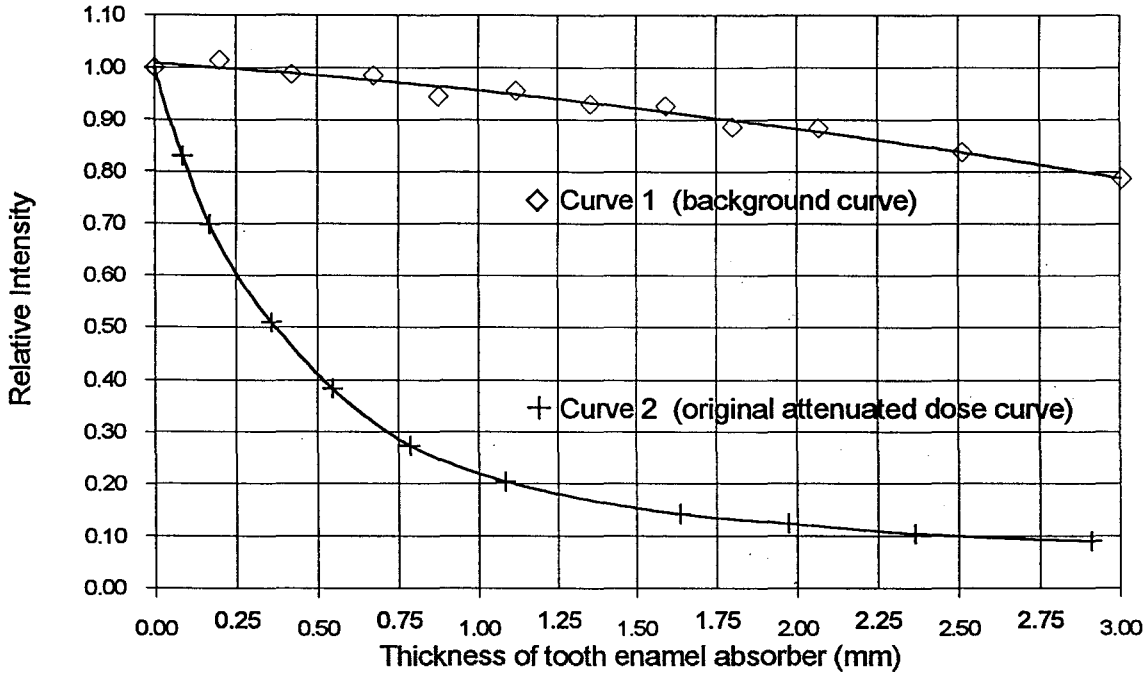

Figure 3.6 Experimental raw data for the pitchblende experiments (with tooth enamel absorber). The "background curve" (curve 1) is obtained by measuring the irradiation field intensity without absorbers, and the "original attenuated dose curve" (curve 2) is obtained by measuring the dose variation with different thicknesses of absorbers.

Experimental results and data processing

In the previous page, the so-called "background curve" (curve 1) and "attenuated dose curve" (curve 2) for tooth enamel absorbers are shown. For aluminum absorbers, a similar curve to curve 2 was obtained, and the data processing is exactly the same.

In order to understand the procedures to reach the final results, first, we have to know what the "background curve" and the "attenuated dose curve" shown in Figure 3.6 actually represent. From the experimental scheme described in the previous part, we realize that the measurement of the "background curve" was intended to describe the distance dependence of the irradiation field without the absorbers, and in Figure 3.6, this curve (curve 1) was described by the following equation:

$$F_1(r)=(D_{\beta 0}+D_{\gamma 0})\times B(r) \quad \text{.....(3.1}a\text{)}$$

where r is the distance between the source and the detector, B(r) is the expression for the normalized background variation (i.e. B(0) = 1), and $(D_{\beta 0} + D_{\gamma 0})$ represents the total dose rate (beta plus gamma) at the surface of the source, but equals unity in the case of normalization, i.e. $D_{\beta 0} + D_{\gamma 0} = 1$, therefore, equation 3.1a can be written as:

$$F_1(r)=B(r) \quad \text{.....(3.1}b\text{)}$$

In these descriptions (equations 3.1a & 3.1b), there is an assumption that the distance dependence of both the beta field and gamma field (in air) follows the same function (i.e.

B(r)), as long as the absorption is negligible for both irradiations. This assumption is theoretically true and practically valid within the distance of 5 mm in the experiment.

The expression for the attenuated dose curve (curve 2) is:

$$F_2(r)=D_{\beta 0}\times f(r)+D_{\gamma 0}\times B(r) \quad \text{.....(3.2)}$$

where r is the distance between the irradiator and the detector, B(r) is the normalized background function (namely, with B(0) = 1), $D_{\beta 0}$ and $D_{\gamma 0}$ are the beta dose rate and gamma dose rate at the surface of the irradiator (without absorption) respectively. f(r), notably, is the beta dose attenuation function which was the aim of this study. Due to normalization, the boundary conditions are: f(0) = 1, $D_{\beta 0} + D_{\gamma 0} = 1$ and B(0) = 1.

In this expression (equation 3.2), there is an implication that the dose measured with absorber is composed of the attenuated beta dose $D_{\beta 0}\times f(r)$ and an unattenuated but distance dependent gamma dose $D\gamma_0\times B(r)$, but the distance dependence of beta dose (in air) is apparently not taken into account. The reason for this is based on the consideration that the actual geometry of the experimental setting was effectively 2-π geometry for the beta irradiation because of the range of beta particles, but not for the gamma irradiation, and in the real 2-π geometry, there is no distance dependence at all for both gamma and beta irradiations. Assuming that the source and absorber are infinitely large, but the detector is the same (ϕ 3mm) as in our experiment, the result of beta attenuation measured must be the same as in our experiment because the effective range of beta particles in tooth enamel

(or aluminum) is only 2-3 mm. Therefore, the background function B(r) is only associated with the gamma dose.

Based on the equations for background and original attenuated dose curve (equations 3.1a,b & 3.2), we can determine the authentic beta attenuation function f(r). This was done by subtracting the gamma background (following the pattern of curve 1) from the original attenuated dose curve (curve 2). However, the key point to implement this subtraction is that the beta dose will be attenuated to almost zero when the absorber is thicker than 2mm, following the pattern of an exponential function, and the gamma background becomes dominant. We can make adjustment to curve 1 (i.e. function B(r)) and obtain the curve of $D_{\gamma 0} \times B(r)$, then we subtract curve $D_{\gamma 0} \times B(r)$ from curve 2 (i.e. function $D_{\beta 0} \times f(r) + D_{\gamma 0} \times B(r)$) to obtain the curve of $D_{\beta 0} \times f(r)$. If we have the function of $D_{\beta 0} \times f(r)$, we virtually know f(r) after a simple normalization, because $D_{\beta 0}$ is just a constant. The criterion for the right adjustment of function B(r) (curve 1) to function $D_{\gamma 0} \times B(r)$ is that after subtraction of the curve $D_{\gamma 0} \times B(r)$ from curve 2, the curve obtained must be exponential and reaching zero with increasing thickness of absorbers. All this analysis is easily explained with the help of the curves shown on Figure 3.7.

The result of the analysis (i.e. the authentic beta attenuation function f(r)) is shown in Figure 3.8. Unit of g/cm^2 was used for the thickness of absorbers (tooth enamel in this graph). If the beta attenuation curve is approximated as exponential, the apparent mass attenuation coefficient (μ/ρ) obtained from the tooth enamel experiment was: 7.46 cm^2/g,

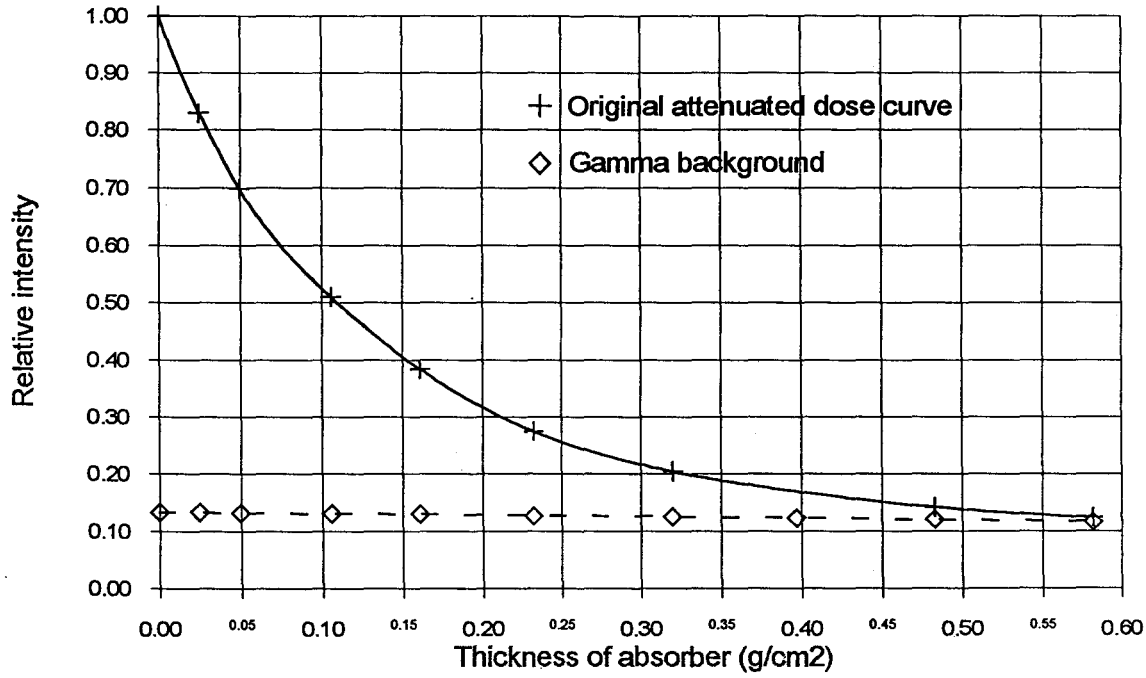

Figure 3.7 Data processing for the pitchblende experiments (tooth enamel absorber). The "gamma background curve" (◇) is derived from "curve 1" in Figure 3.6 (see text for details). The "original attenuated dose curve" (✚) is the same as that in Figure 3.6. Subtracting the gamma background from the original attenuated dose curve will yield the beta attenuation curve. (see Figure 3.8)

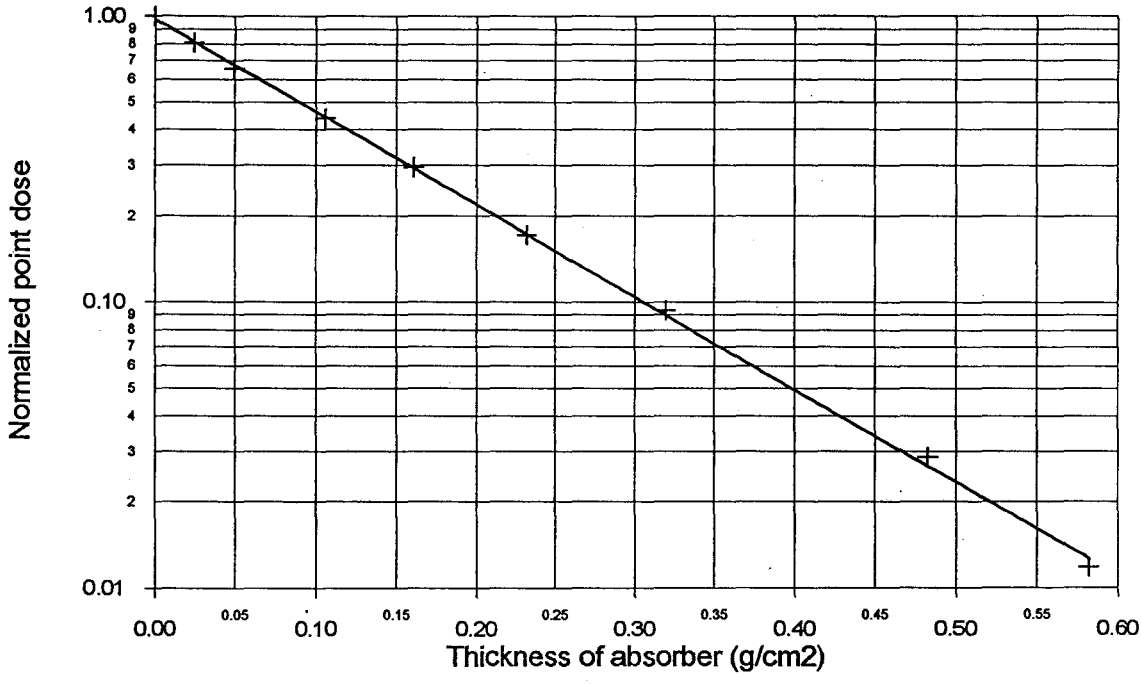

Figure 3.8 Beta attenuation curve (dose-depth variation curve) obtained from the pitchblende experiments(for tooth enamel absorber). The solid line shown in the graph is the exponential fitting line. The mass attenuation coefficient (μ/ρ) obtained is 7.46 cm^2/g, which corresponds to a μ value of 2.20 mm^{-1} for tooth enamel absorber.

and it corresponds to an attenuation coefficient (μ) of 2.20 mm^{-1} for tooth enamel and 2.01 mm^{-1} for aluminum, which is much higher than that achieved by Aitken et al. (Their μ value for the pitchblende experiment was 5.7 cm^2/g, or 1.68 mm^{-1} for tooth enamel). The result for aluminum absorber is approximately the same as that achieved in the tooth enamel experiment, and the mass attenuation coefficient obtained in this experiment is 6.95 cm^2/g (namely, μ=2.05 mm^{-1} for tooth enamel), which is also much higher than Aitken et al.'s.

3.1.3 Analysis of the two experiments

The experiment of Aitken et al. and our experiments using pitchblende all support the prediction that the beta attenuation in 2-π geometry is approximately exponential, but they revealed different attenuation intensities, indicated by their different μ values. Figure 3.9 is a comparison of our experimental result with Aitken et al.'s in the form of dose-depth variations. (From our experiments, only tooth enamel data are shown.) The difference between these two curves clearly reflects the difference between the theoretical predicted curves by Grün's approximation and "one group" theory, as shown previously in Figure 2.10.

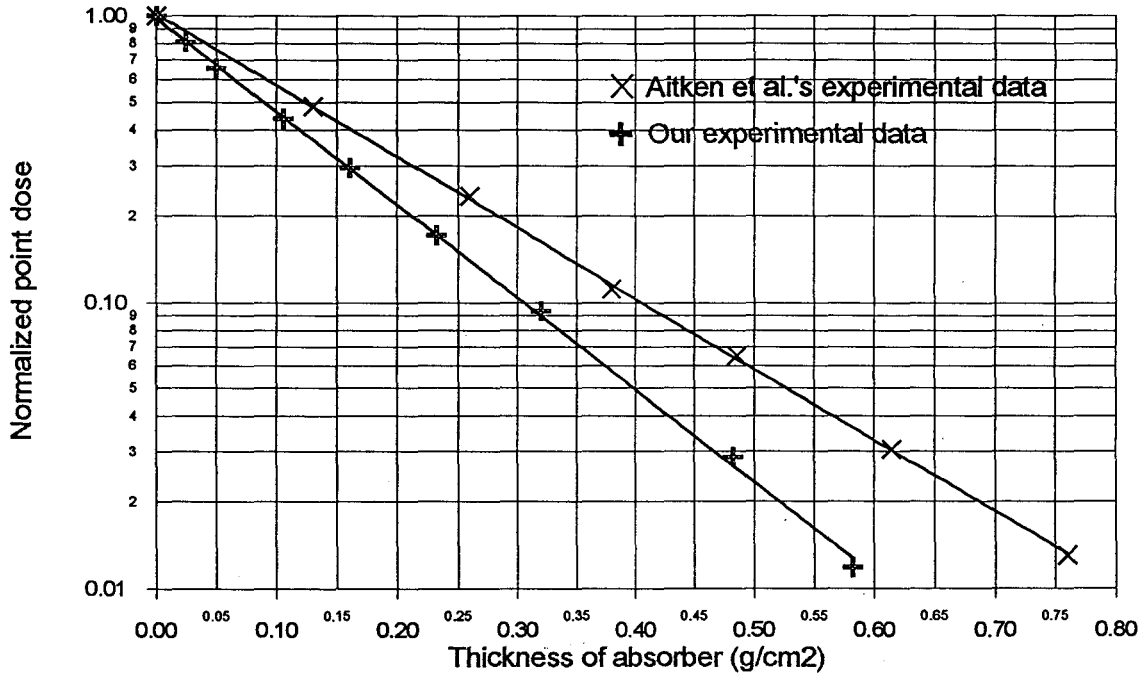

Figure 3.9 Comparison of our experimental result (for tooth enamel) with Aitken et al.'s result in the form of dose-depth variation. Both best-fitting lines are exponential.

Discussion of 2-π geometry

The difference between our experimental results and Aitken et al.'s results is conspicuous, and beyond the range of any possible errors, so there must be an explanation for this contradiction. As far as I can see, the problem originates in the geometric difference between these two experimental settings, and I believe that there is an apparent violation of 2-π geometry in Aitken et al.'s (1985) experimental arrangement which can be seen in Figure 3.1.

The key feature of their experimental arrangement is that they kept the distance between the irradiator (pitchblende surface) and detector (TL phosphor) constant to avoid the variation of gamma background. However, with the change of the absorber thickness, the distance between the lower surface of the absorber and the detector was changed dramatically (refer to their experimental setting in Figure 3.1). If the experimental setting cartoon they presented in the paper is in the correct proportional scale, the distance between the irradiator and detector was kept 12.5 mm apart. When they changed the thickness of their absorber from 0 to 5 mm, the distance between the lower surface of the absorber and the detector was changed from 12.5 mm to 7.5 mm, and the angle associated with this change was from 106^0 to 128^0 (refer to Figure 3.1), which is clearly not 2-π geometry (i.e. 180^0). Their violation of 2-π geometry well explains the discrepancy between our experiments and their experiments.

As a matter of fact, their experimental arrangement was destined to result in a weakened attenuation effect as was shown in their results, because, with increasing absorber thickness, the angle between the absorber and detector was also increasing, and that would anomalously enhance the dose recorded by the detector (for thicker absorber) and lead to the observation of apparently weaker attenuation.

In our experiments, however, both the relationship between the source and absorber and the relationship between the absorber and detector are close to 2-π geometry. The variation of gamma background was circumvented by the measurement of the variation of the overall irradiation field. The minor uncertainties introduced by the background subtraction were a common problem shared by these two experiments (Aitken et al.'s and ours), which led us to the second set of experiments using the $^{90}Sr(^{90}Y)$ source, with the experimental configuration of using tooth enamel pellets as both absorber and detector.

Conclusion

Based on the analysis above, we conclude that: 1) departure from 2-π geometry in Aitken et al.'s (1985) experiments led to a beta attenuation curve with anomalously low μ value, and 2) our experimental results support the "one group" theory and Monte Carlo beta attenuation calculations rather than those of Grün's approximation. (1986)

3.2 Beta attenuation determination using $^{90}Sr(^{90}Y)$ as the irradiator

3.2.1 Experimental design

In this second set of experiments, we employ a $^{90}Sr(^{90}Y)$ plate source and a stack of detectors (tooth enamel pellets) which ensures near-perfect 2-π geometry (Figure 3.11). In order to fulfill the requirement of electron equilibrium during the irradiation, which is very important to simulate the actual irradiation conditions, we also made a "holder" of solid fossil tooth enamel to surround the pellets. This design allows us to record the beta attenuation directly within the tooth enamel, which is an ideal analogue to the natural irradiation geometry.

Materials for the experiments

The source we employed in our experiments is a planar ^{90}Sr source manufactured by Amersham (U.K.), in 1959, with radioactive area of 10 mm × 10 mm and nominal activity of approximate 4 mCi. The source is believed to be coated on a silver/steel plate, which was the standard manufacture of the time. Strictly speaking, the ^{90}Sr source we employed should be designated as a $^{90}Sr(^{90}Y)$ source because there are two decaying elements in the source. ^{90}Sr is the parent, and^{90} Y is the daughter. Both of these two radioactive elements are beta (negatron) emitters, with half lives of 28.5 years and 2.67 days respectively. The average energy of beta particles emitted by ^{90}Sr is about 196 keV, and the average

energy for ^{90}Y beta decay is 934 keV. (Their energy spectrum are shown in Figure 2.3) Generally, these two elements are at radioactive equilibrium, so the $^{90}Sr(^{90}Y)$ source is often considered as a double beta decaying source with equal contributions from both ^{90}Sr and ^{90}Y. (Note that there are no gamma rays produced in the decays of either ^{90}Sr or ^{90}Y.) In the theoretical calculations discussed previously, this property of the source is taken into account.

The material for making the pellets was pure tooth enamel powder (grain size < 75 mm by sieving) obtained from a modern bovid tooth (found on the campus of McMaster University by Ken McDonald). The reason for choosing a modern tooth is actually critical because there must be virtually no background dose in the tooth enamel pellets, for the sake of better detection of the relatively weak beta dose received from the ^{90}Sr beta source. To ensure that there was no background dose in the tooth enamel for making pellets, we experimentally determined the accumulated dose in the modern tooth enamel, by the "additive dose method" (Grün, 1989). The dose response curve is shown in Figure 3.10. The signal intensity before irradiation is near zero, as needed for the experiment.

The tooth enamel holder was cut from the same large fossil mastodon tooth, which was used for making the tooth enamel absorbers in the previous "pitchblende" experiments. The very thick (~ 5mm) and large (~ 12mm × 12mm) piece of tooth enamel was then carefully ground and polished to make the surface flat and precisely even, by applying the device we developed to grind the absorbers in the previous experiment. (See Figure 3.12 for the picture of the holder.)

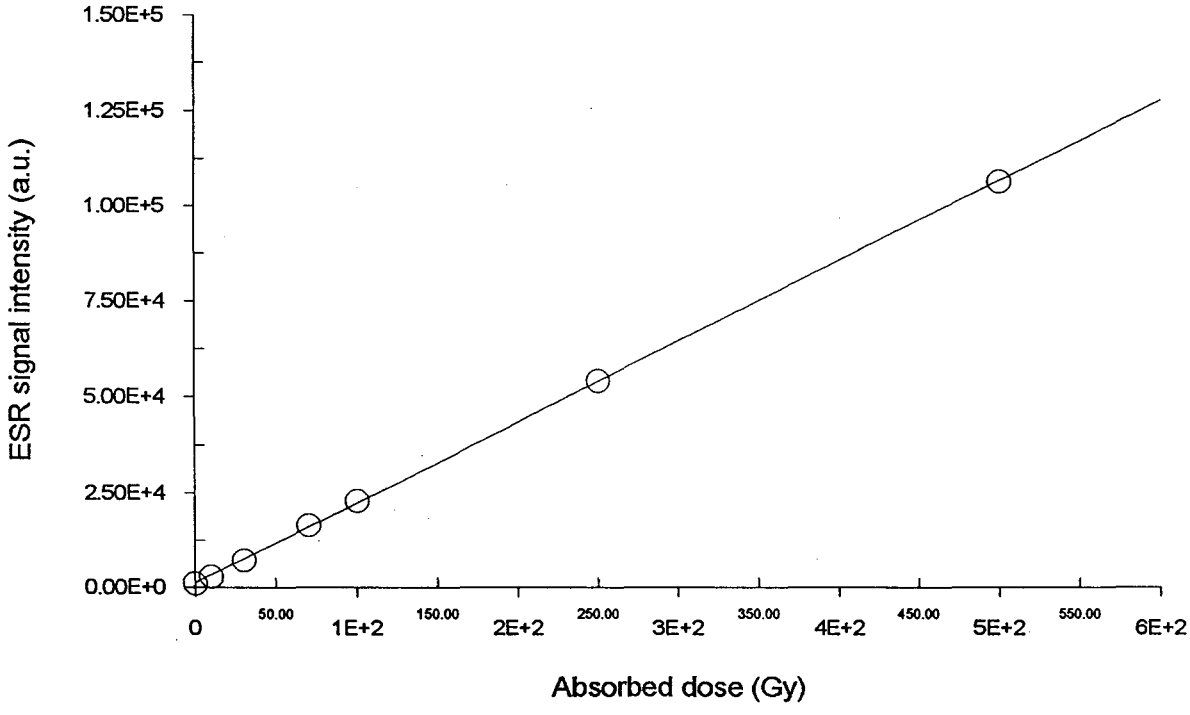

Figure 3.10 The dose response curve for the tooth enamel powder for making pellets. The best fitting line is linear, in the range of 0-500 Gy (maximum artificial γ-dose).

In order to match the dimensions of the $^{90}Sr(^{90}Y)$ plate source (10mm×10mm), the tooth enamel pellets were made into 4.8 mm in diameter, with thickness ranging from 100 μm to 300 μm, using a standard pellet presser with pressure of about 8,000 pounds for 1 minute. The hole cut into the solid tooth enamel holder is 3 mm deep and 4.8 mm in diameter, using a lathe. For better resolution of the dose distribution, it was desirable to make the thinnest possible pellets. We started using 300 μm thick pellets and eventually were able to make them as thin as 120 μm.

Experimental setting

As shown in Figure 3.11, the tooth enamel pellets were tightly stacked into the hole of the solid tooth enamel holder until the hole was fully filled and the surface of the last pellet was exactly at the same level of the surface of the holder. The planar $^{90}Sr(^{90}Y)$ source was then placed directly on top of the tooth enamel holder centered over the pellets stack. In order to avoid radioactive contamination, a very thin piece of mylar (3 μm thick, or 0.00051 g/cm^2) was used to separate the source and the tooth enamel assembly. The absorption caused by this thin layer is negligible.

The relationship between the planar source and the tooth enamel layer is a very close approximation to 2-π geometry. Considering that the beta range is only about 2mm in tooth enamel, it is quite safe to say that the doses received by the tooth enamel pellets in the middle of the tooth enamel holder well represent the beta attenuation pattern for ^{90}Sr

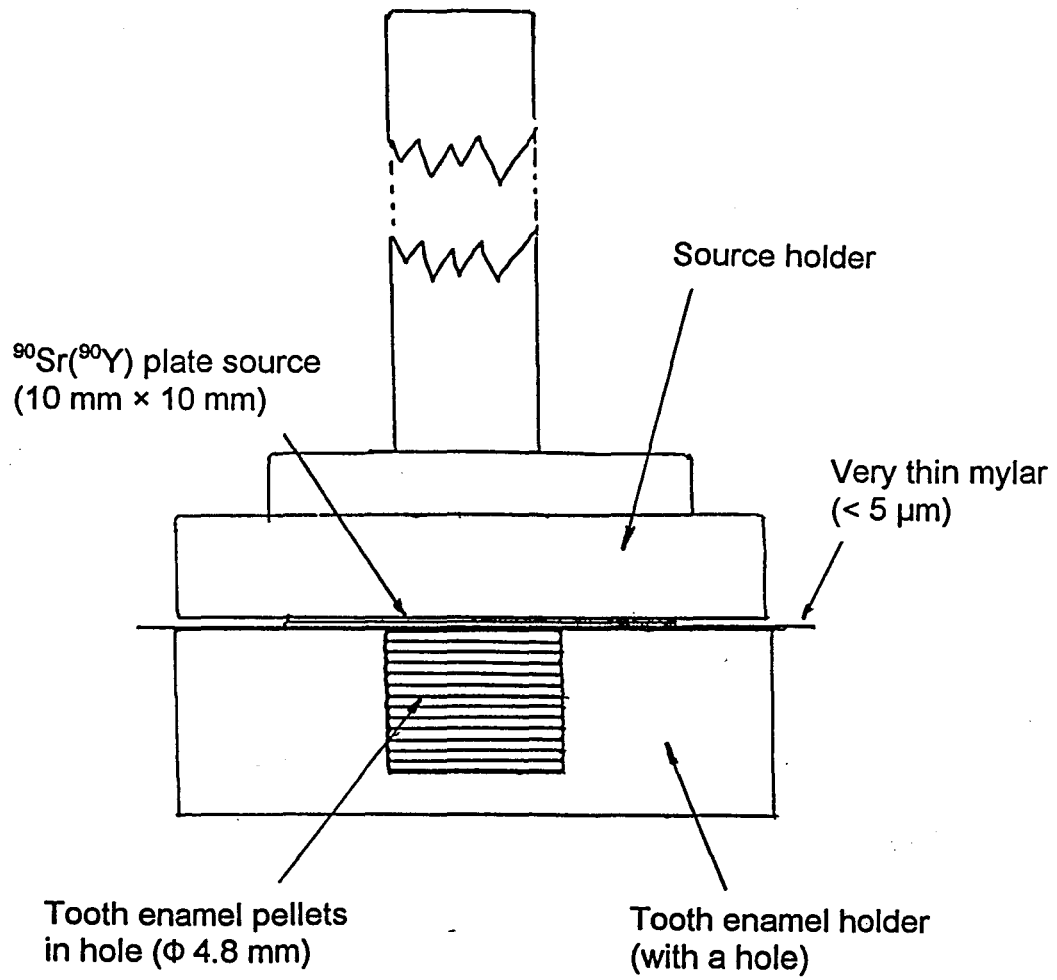

Figure 3.11 Experimental configuration for the experiments using ^{90}Sr(^{90}Y) source as the irradiator. (refer to the text for details)

source under 2-π geometry.

Figure 3.12a shows some of the tooth enamel pellets and the holder used in the experiments with the ^{90}Sr source. Figure 3.12b shows the pellets in the holder and demonstrates the flatness of the composite arrangement, which is very critical for 2-π geometry and electronic equilibrium. Because both the absorber and detector were made of tooth enamel, and the dose measurement was done by the method of ESR, all the disadvantages associated with using external detector are avoided, especially the problems of energy dependence of the detector.

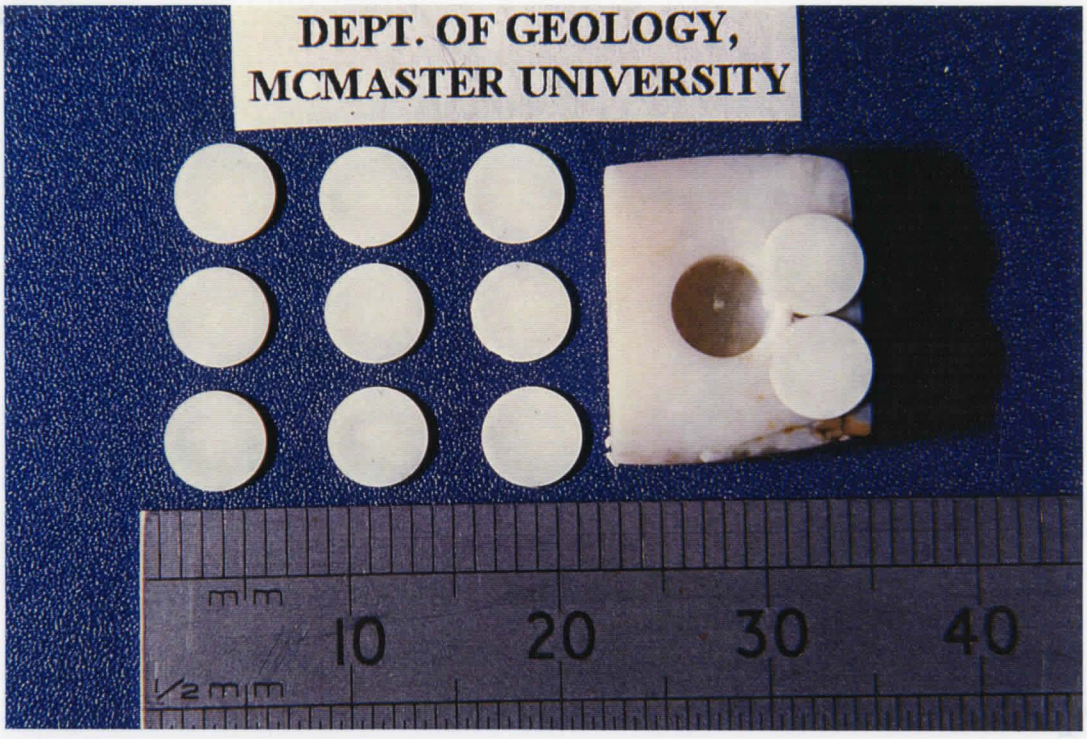

Figure 3.12a Picture of some tooth enamel pellets and the tooth enamel holder

Figure 3.12b Picture of the pellets in the hole of the holder

3.2.2 Experimental results

The intensity of the ESR signal is a good indicator of dose absorbed in the material, however, the ESR signal is not always strictly proportional to the dose absorbed. Saturation would have occurred if the dose absorbed in the material is too high. For the direct measurement of beta dose attenuation, we ensured that there was no saturation occurred in all of the pellets being irradiated through an earlier gamma dose irradiation experiment. (Figure 3.10) There was little background dose in the pellets, and the dose-signal response was linear in the range of 0-500 Gy. During the beta irradiation, the maximum dose received by the first pellet (closest to the source) was kept below 500 Gy (equivalent of gamma dose), ensuring that the ESR signal of each pellet directly represent the beta dose it absorbed.

First run

The pellets made for the first attempt of the experiment were weighed about 10 mg each, and were about 220 μm thick. Thirteen pellets were used and subjected to a 2 hour irradiation (about 160 Gy equivalent gamma dose to the closest pellet), under the arrangement shown in the experimental setting (Figure 3.11), then measured one week later. The ESR measurement conditions are: microwave power: 0.635 mw; modulation amplitude: 5 Gauss; modulation frequency: 100 kHz and the gain for all measurements was kept at 2×10^5. The pellets were broken into pieces for the measurements and measured in a 3 mm inside diameter fused quartz tube. Each pellet was measured twice in different orientations

and scanned 3 times in each case in order to detect any directional variation of ESR signal. Fortunately, the variation of ESR signal due to orientation was very small, because the starting material for the pellets was powdered, and the pellet press pressures had not introduced any preferential alignment of grains. The final ESR signal intensity for each pellet was taken to be the average of several measurements.

All of the pellets were measured successively, and the dose-depth variation curve was obtained by plotting the data points on a graph of "absorber thickness" (in g/cm^2) versus the "relative dose", i.e, the doses of subsequent pellets divided by the dose of the first pellet. The data are shown in Figure 3.13, along with comparison of the theoretical predictions. The error bars shown in the experimental data points represent 2 times the standard deviation (96% of certainty) of ESR measurements, which was obtained by measuring one of the sample aliquot in the set for 12 times. (same in the following results.)

The first attempt of the experiment was successful, although there was some departure from the expected result (i.e. "one group" theory's prediction) for the pellets nearest to the source (refer to Figure 3.13). This might be due to the experimental arrangement because, during the irradiation, the pellet nearest to the source was slightly above the "holder" surface and therefore lost some of the beta dose scattered from the matrix and led to the depression of the first pellet dose. Since all other doses were normalized to this data point, this would enhance the relative doses of the lower pellets. Nevertheless, the initial results tend to support the beta attenuation calculations using "one group" theory.

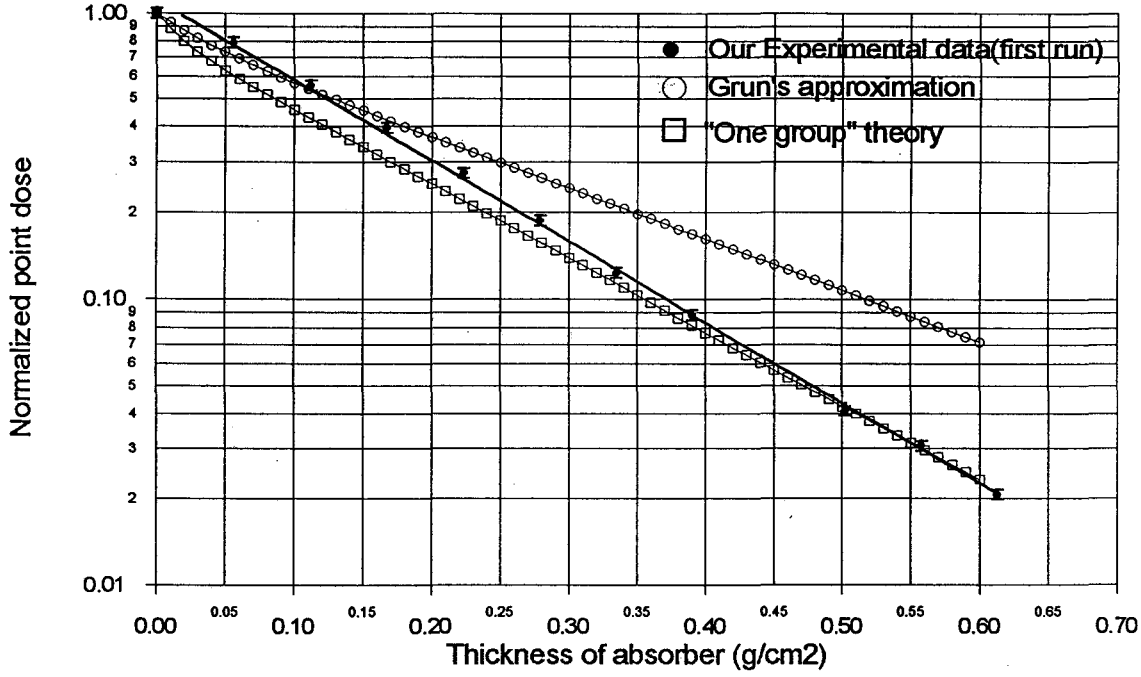

Figure 3.13 Dose-depth variation for $^{90}Sr(^{90}Y)$ source (comparison of the theoretical predictions with our experimental result of the first run).

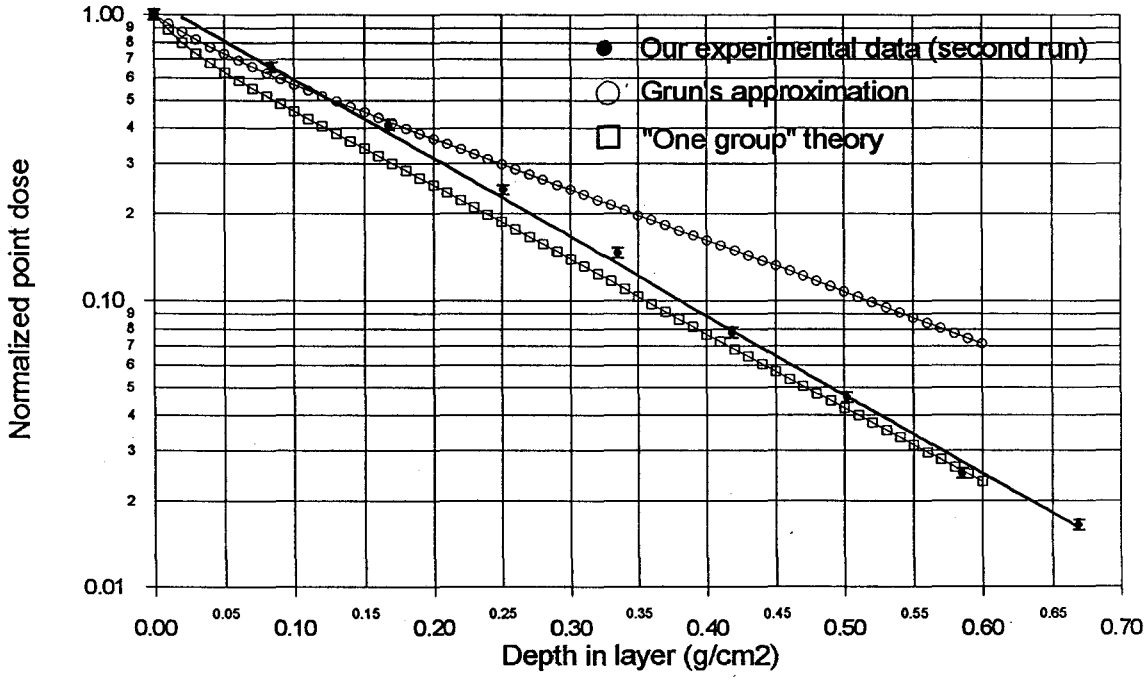

Figure 3.14 Dose-depth variation for $^{90}Sr(^{90}Y)$ source (comparison of the theoretical predictions with our experimental result of the second run).

Second run

The second run of the experiment was done to see if the results of the first experiment could be reproduced. The pellet's thicknesses were even thicker because they were made earlier than those in the first run and were originally made as spares. The mass of each aliquot for each pellet was about 15 mg, and the average thickness of the pellets was 330 μm. Altogether, nine pellets were stacked into the hole of the tooth enamel holder and were then irradiated by the ^{90}Sr plate source, following the procedures described in the first run. The irradiation time was 5 hours which delivered about 400 Gy (equivalent to gamma dose) to the first pellet. After the same data processing as in the first run, we obtained a dose-depth variation curve which is shown in Figure 3.14. This time the first part of the curve seems to be more exponential and fit well to the "one group" theory prediction. The result of the second run confirms the previous experiment and supports the "one group" prediction, but, as in the first run, deviates significantly from the theoretical curve near the origin.

Third run

The results from the first and second run are in good agreement with the "one group" theory, especially for larger absorber thicknesses. However, in order to obtain a better understanding of the beta attenuation curve for smaller thicknesses, we carried out a third run of the experiment, with even more careful procedures and even thinner pellets at the top of the hole. Six pellets of 5 mg each were made, which were about 120 μm thick.

Another eight pellets of 10 mg each were stacked below the thinner pellets. The whole set was irradiated for 5 hours (~ 400 Gy for the first pellet) by the source. The ESR signal intensity of each pellet was measured and normalized by its mass. Following the same procedure as described in the previous runs, the dose-depth variation was plotted in Figure 3.15, together with the theoretical predictions. As expected, the attenuation curve fits better with the theoretical prediction, presumably because of the higher resolution at thinner absorbers. All three runs of the experiments using $^{90}Sr(^{90}Y)$ source showed excellent reproducibility and agree with the "one group" theory's prediction, while deviating significantly from the prediction of Grün's approximation.

Qualitatively speaking, the results presented above are correct, however, in the strict sense, we have to consider the errors introduced by the thickness of the pellets, which, in the above discussion, were treated as having zero thickness. In fact, the dose recorded in the first pellet (nearest to the source) is the average dose within the thickness of the pellet, which is 120 μm thick in the third run, but in the theoretical predictions, the first point is for the dose ultimately adjacent to the source, which can not be experimentally determined. To solve this discrepancy, we can use the theoretical calculations to predict the average dose in each pellet (whose thickness is known), and compare the experimental results directly with their counterparts. This idea is fulfilled by integrating the theoretical curves in segments, which correspond to the segments of stacked pellets. Finally, the calculated average doses for all pellets are plotted in the same way as for the experimental data. The result is shown in Figure 3.16 (for the third run only). Without question, the experimental results achieve

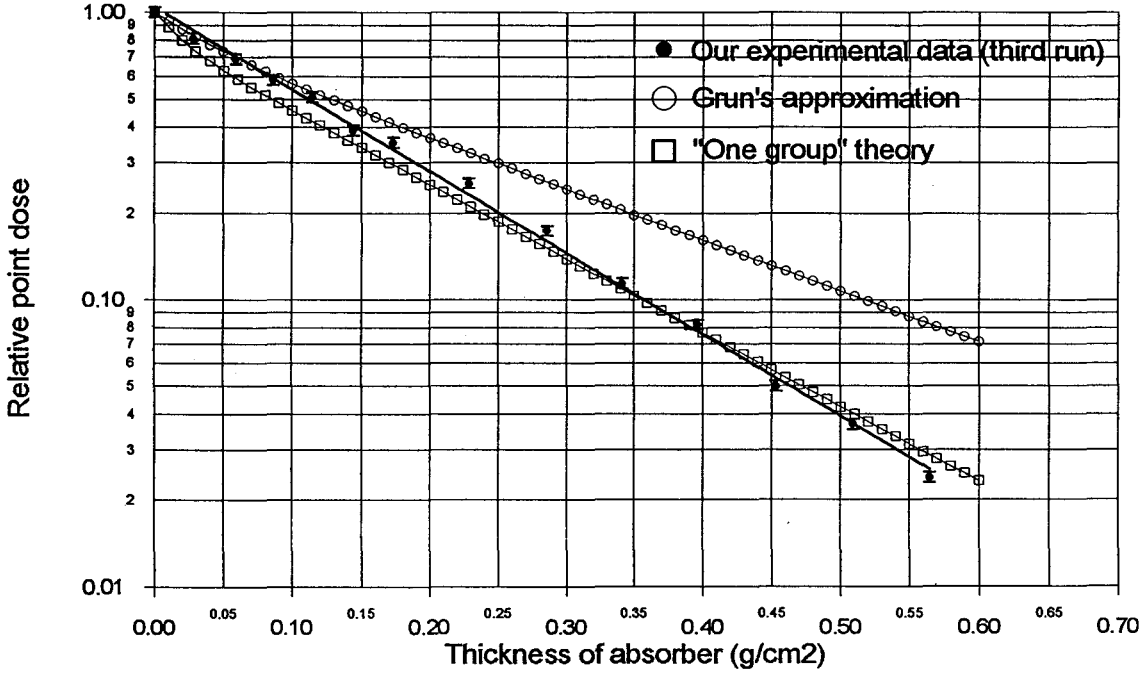

Figure 3.15 Dose-depth variation for $^{90}Sr(^{90}Y)$ source (comparison of the theoretical predictions with our experimental result of the third run).

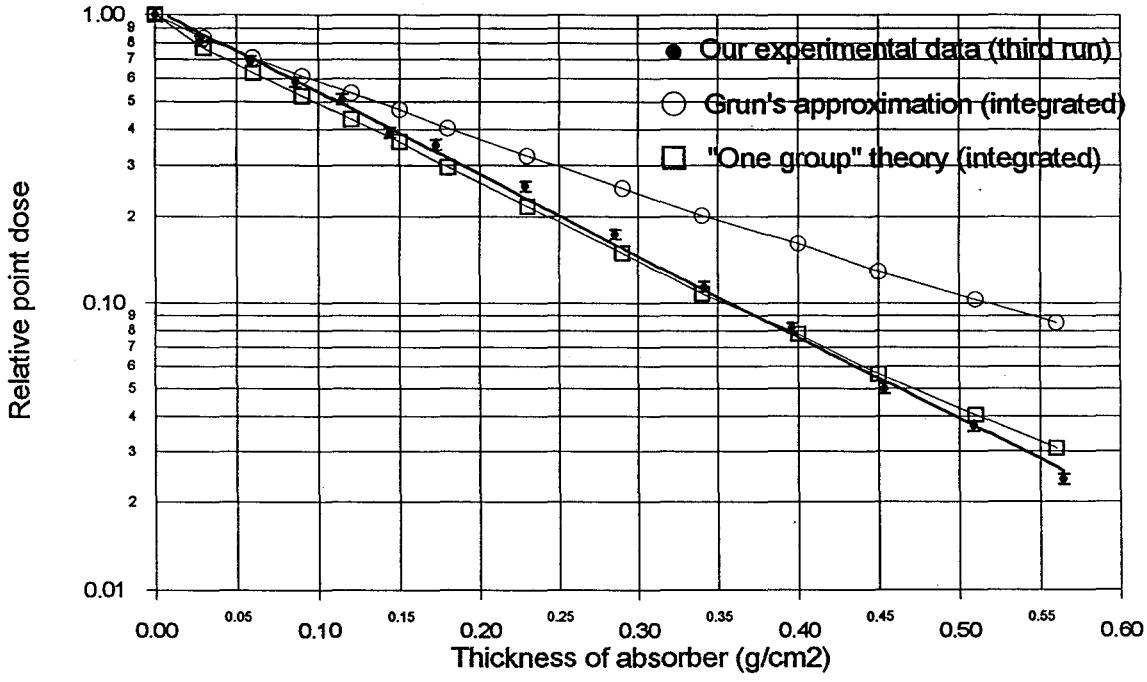

Figure 3.16 Comparison of our experimental results (third run) with the theoretical predictions, which are segmentally integrated for estimating the average doses of individual pellets. (refer to the text for details)

even better agreement with the prediction of "one group" theory.

3.2.3 Discussion

From the experimental results presented above, we conclude that the "one group" theory's calculation is more accurate than Grün's approximation. Although the experimental curves show lower attenuation at the beginning (i.e. higher relative ESR intensities for pellets near the source), the majority of the data support our interpretation. The reason for this departure at low thickness might be due to the fact that the plate $^{90}Sr(^{90}Y)$ source we used was coated on a silver/steel backing which has a very high Z number, and the "one group" theory's prediction was based on the preassumption that the radioactive source is in a uniform half space of silica containing the radioactive elements. Analytically, higher Z number may result in higher energy backscattering, so the beta particles backscattered from the steel plate of the source into the tooth enamel absorber are more energetic than those from the presumed silica. Higher energetic beta particles are more penetrating and thus may explain the phenomenon of weaker absorption at shallow absorber than theoretically predicted. Anyway, these deviations could be better understood if more detailed calculation (that incorporates the effects of silver/steel back plates) was done. This extended topic was not addressed, however, our experimental results strongly support the prediction of "one group" transport theory and meanwhile contradict Grün's (1986) approximation and Aitken et al.'s (1985) experimental results.

3.3 Summary of the experimental work and its conclusions

Two series of experiments were carried out in this project to address the beta attenuation problem. One employs the similar experimental arrangement as that of Aitken et al.'s (1985), which used the irradiator-absorber-detector configuration. This group of experiments were aimed to compare the experimental results directly with those of the previous experiments, although the experimental design was not ideal considering the possible uncertainty induced by background subtraction and the geometric problems. Nevertheless, the results of our experiments show clear inclination to the "one group" theory's prediction and are far away from the expectation of Grün's approximation. This gives us confidence that the "one group" theory is more accurate in beta dose calculation. Moreover, with careful study of Aitken et al.'s (1985) experiments, we conclude that their experimental arrangement deviates from 2-π geometry, which may explain the observed weaker beta attenuation.

In order to strengthen our argument and avoid the possible uncertainties introduced by the mathematical manipulation in data processing, we designed another series of experiments employing a pure beta source (^{90}Sr), and an enamel holder containing tooth enamel pellets which is fundamentally different from the configuration of irradiator-absorber-detector. This is true 2-π geometry, with the enamel pellets acting both as detector and absorber. The doses recorded in the tooth enamel pellets were detected by ESR spectrometry, which is exactly the same method employed in ESR dating. There were very few

mathematical manipulations involved in the data processing and the attenuation curves were achieved by directly plotting the experimental data in the graph (after normalization). This simple approach yielded results which clearly support the "one group" theory.

To sum up, we have gathered three pieces of evidence to support our conclusion that the "one group" theory of beta dose calculation is correct: 1) Aitken et al.'s (1985) experiments, which are the cornerstone for Grün's approximation of beta dose calculation, were found to be problematic because of a flawed experimental geometry, and this explains the reason why their beta attenuation curve is significantly different from "one group" theory and Monte Carlo calculations; 2) our experiments using the same configuration of irradiator-absorber-detected as employed in Aitken et al.'s experiments gave results to support "one group" theory's prediction, after careful treatment of the gamma background and circumvention of non-2π geometry; 3) our experiments employing tooth enamel pellets essentially solved the problems related to the irradiator-absorber-detector arrangement, and the results of these experiments also strongly support the prediction of "one group" theory.

With all the three evidences listed above, we are quite confident to conclude that the theoretical prediction of beta dose by "one group" theory is more reliable than that of Grün's approximation, thus the ESR ages calculated by Grün's approximation should be revised accordingly.

CHAPTER 4

IMPLICATION OF OUR EXPERIMENTAL RESULTS IN ESR DATING OF TOOTH ENAMEL

Comparatively speaking, the ESR dating technique is a complex topic, and the beta dose calculation is only part of the subject related to the dose rate estimation, however, it is very important. As indicated previously, different speculation about the beta dose assessment can result in a large difference in the final ESR ages, and such perception is practically implemented by the performance of two different computer programmes: DATA and ROSY. The DATA programme is a well accepted computer software in the field of ESR dating and numerous ESR ages were published, based on the calculation of this programme. Our experimental results, however, firmly support the ROSY prediction, and consequently challenge all the old ESR ages calculated by the DATA programme. That will inevitably have a great impact on ESR dating.

4.1 General impacts on ESR age calculation

Fundamentally, the main difference between the two ESR age calculation programmes (DATA and ROSY) is that of the beta attenuation in sample materials, which is

particularly addressed in this thesis. (There are some minor differences in alpha dose and cosmic ray dose calculations, but their influence is relatively small.) However, this disagreement results in up to 50% difference of average beta dose received by the sample from the same external source. DATA's prediction of external beta dose is always higher than that of ROSY. Generally, in the case of tooth enamel, the external beta dose consists of up to 30% of the total dose the sample receives, thus the average age difference calculated by these two different computer programmes would be approximately 15%, based on the perception that the age difference is inversely proportional to the difference of dose rate calculated.

The general impacts of our experimental results on ESR dating can be illustrated by the intercomparison of ESR ages calculated by these two different computer programmes (DATA and ROSY) based on the same input data, which are from actual ESR dating samples (from a variety of sites). Table 4.1 (Brennan et al., 1997) displays the raw input data for the age calculation. Table 4.2 shows the output data of the two computer programmes. The calculated ESR ages, both EU (early uranium uptake model) ages and LU (linear uranium uptake model) ages, are given. The total dose rate and individual dose rate (α-, β-, γ- and cosmic rays) values are also obtained by computation.

Table 4.1 Input data for ROSY and DATA software intercomparison

Sample	Enamel thickness (μm)	Outer enamel removed (μm)	Inner enamel removed (μm)	Accumulated dose (AD) (Grays)	Enamel Uranium (ppm)	Dentine Uranium (ppm)	Sediment Uranium (ppm)	Sediment Thorium (ppm)	Sediment Potassium (wt,%)	Sediment moisture (wt.%)	Burial depth (m)
1	1828 ±360	50±25	44±22	162.9±2.7	0.22±0.1	63.8±0.1	1.60±0.19	6.92±1.36	0.78±0.13	10.0±10.0	4.3±0.13
2	697±76	62±31	44±22	34.0±3.3	1.18±0.1	23.4±0.1	1.65±0.12	2.06±0.08	0.12±0.01	12.9±2.8	1.0±0.5
3	775±108	40±20	40±20	70.9±2.7	3.92±0.1	148.4±0.1	6.94±3.84	1.06±.20	0.14±0.03	10.0±10.0	4.0±1.0
4	1129±67	54±27	39±20	147.1±2.9	6.22±0.1	186.4±0.1	1.56±0.1	6.27±0.18	0.67±0.04	14.0±10.0	3.0±2.0
5	968±71	54±27	48±27	747.1±80.4	26.0±0.1	32.6±0.1	0.97±0.1	4.48±1.48	1.57±0.12	10.0±10.0	80.0±20.0
6	1020±132	41±20	49±25	25.5±0.7	<0.1	0.15±0.1	3.09±0.1	8.19±0.46	0.52±0.03	20.0±10.0	N/A

Footnotes:

N/A = not applicable (see Table 4.2)

Burial depths are used to calculate cosmic dose rates in Table 4.2

Table 4.2 Output data for ROSY and DATA software intercomparison

Sample	Sediment γ dose rate (μGy/a)	Cosmic dose rate (μGy/a)	Sediment β dose rate (μGy/a)	Dentine β dose rate (μGy/a)	Enamel α+β dose rate (μGy/a)	Total dose rate (μGy/a)	EU age (ka)	LU age (Ka)	CU age (Ka)	Enamel α dose rate (μGy/a)	Enamel β dose rate (μGy/a)
ROSY											
1	657	89	78	556	72	1452	112±12	145±16	139±15	60	12
2	282	147	67	351	229	1076	32±3	44±4	37±3	195	34
3	787	93	185	1991	664	3720	19±3	30±6	25±4	559	105
4	574	109	108	2092	1266	4149	35±2	59±3	45±3	1070	196
5	651	0	210	612	7654	9127	82±7	144±12	84±7	6288	1426
6	530*	**	122	2	0	654	39±5	39±5	39±5	0	0
DATA											
1	650	119	116	953	68	1838	86±8	118±11			
2	278	183	87	484	219	1251	27±3	38±4			
3	781	124	254	2786	634	4579	15±2	25±4			
4	563	140	147	3094	1223	5167	28±1	48±2			
5	643	0	273	726	7465	9107	82±12	144±20			
6	530*	**	168	3	0	701	36±5	36±5			

Footnotes:

1. All calculation were done using 0% water in dentine and enamel
2. Cosmic dose rates for DATA and ROSY are based on the work of Prescott and stephan 1982

* Value is sediment gamma plus cosmic dose rate determined by thermoluminescence dosimetry

** Included in sediment gamma dose rate for this sample

Comparing the results in detail, we find out that the ROSY calculated ages are generally much older than the DATA calculated ages (both EU and LU). The ratio of ESR ages obtained by ROSY vs. DATA ranges from 1.0 to 1.30 for early uranium uptake model (EU) and 1.0 to 1.23 for linear uptake model (LU). Sample 1 shows the extreme case that the ROSY age (EU) is 30% older than DATA age (EU), and by comparing the individual dose rates, we notice that in this sample the external beta dose rate (dentine + sediment) plays a dominant role in the total dose rate while the internal α-dose is minor. This explains the large difference between DATA and ROSY ages since their major difference is in the beta dose calculation. In the case of lower uranium concentration in tooth enamel and higher uranium concentration in dentine and sediment, the ROSY ages are always much higher than DATA ages, as shown by the samples 1, 2, 3, 4 and 6, based on the same reason explained for sample 1. In sample 5, the internal α- and β- doses are so large that the difference in calculated external beta doses makes almost no difference in the ages.

The data discussed above represent the general cases in ESR dating of tooth enamel, because they are examples chosen from a large number of real dating samples to cover the extent of difference between DATA calculation and ROSY calculation. To further illustrate the significance of our experimental data, a comparison of published ages based on DATA calculation will be recalculated using ROSY programme.

4.2 Challenge to the old ESR ages

The DATA programme has been widely accepted as a tool in ESR dating since the time it appeared several years ago. The software was well developed and quite flexible in dealing with different kind of ESR dating samples, especially for ESR dating of tooth enamel. Whereas the principles of the DATA programme are considered to be a significant achievement in the field of ESR dating, its reliability (excepting the beta attenuation algorithm) has not been challenged. Many age calculations in ESR dating were accomplished by this computer programme due to its popularity and accessibility. The ROSY programme, in contrast, is a newly developed ESR age calculating programme, aimed to provide new version of beta dose calculation. However, with all the discussion above, it is clearly shown that the ROSY's version of beta dose calculation is correct and the DATA's prediction is further away from the experimental fact, consequently, we believe that the ESR age calculated by ROSY is more reliable than that obtained by DATA, and many ESR ages using the DATA programme have to be revised using the ROSY programme.

To start the revision, I selected two groups of samples (Chen, et al., 1994, Chen, et al., 1997) with which I am quite familiar because of my direct involvement in the original ESR dating studies.

In 1984, a well-preserved skull of an early form of *Homo Sapiens* was unearthed

from Pleistocene cave deposits at the Jinniushan site in China. Following the discovery, much work was done to estimate its age, especially by the method of uranium series dating, and finally, an age of 230-300 kyr was assigned to this skull based on the accumulated ages of U-series dating. (Chen & Yuan, 1988) This age put the Jinniushan skull among the oldest *Homo Sapiens* material found in China, and raised the possibility of the coexistence of *Homo Sapiens* and *Homo Erectus*. In order to cross check the Uranium series ages, beginning in 1989, the ESR dating method was also employed to address this important site, because it was the only other appropriate method to determine an age as old as several hundred thousand years old. Five tooth enamel samples from Jinniushan site were carefully studied, and after detailed research, including the measurement of some basic parameters, such as the alpha efficiency (K_α value) and the radon loss level, etc, the work reached a conclusion that the average age of the five tooth enamel samples studied was 187 kyr, which was considerably lower than the uranium series ages, however, it was within the expectation of archaeologists. Owing to the importance of the skull and its remarkable age, a paper was published. (Chen, et al., 1994)

The computer software we used to calculated the ESR ages was DATA, which was the only well-accepted programme at that time. The following table (table 4.3) gives a comparison of the ESR ages calculated by DATA and ROSY programmes, based on exactly the same raw data for the five Jinniushan tooth enamel samples.

Table 4.3 Comparison of ESR ages calculated by ROSY and DATA (Jinniushan *Homo Sapiens* Site, China)

Sample number	DATA calculated ages (ka)	ROSY calculated ages (ka)
y91001	192 ± 23	242 ± 32
y91002	165 ± 20	207 ± 26
y91003	195 ± 23	241 ± 30
y84070	193 ± 23	226 ± 29
y84071	188 ± 22	215 ± 27
Mean ± STD	**187 ± 22**	**226 ± 29**

From the table we see that the original ESR ages calculated by DATA programme have an average of 187 ± 22 kyr ("EU" ages, the uranium closed system was tested and reported in the paper), (Chen et al., 1994) and the ROSY calculation gives an average age of 226 ± 29 kyr (also "EU" ages). The difference between these two average ages is 21%. The reason for this large difference is because the five tooth enamel samples we studied are all sandwiched between two layers of dentine (or cement), and the uranium concentration in dentine (or cement) is much higher (about 60 ppm in average) than that in the tooth enamel (average 1.5 ppm). As we discussed previously, this situation will lead to the domination of external beta dose and that yields the difference between DATA calculation and ROSY calculation. Although the revision is so large, the recalculated ages actually prove our original suspicion that the ESR ages must be consistent with the uranium series ages, and after ROSY revision, the ESR ages are almost the same as the ages (230 - 300 kyr) achieved by U-series dating. This outcome seems to strengthen our confidence again that the ROSY's calculation of ESR ages is more reliable.

The other group of samples I have chosen to do the revision are from a recent paper published in *Quaternary Science Reviews*, 1997, (Chen et al., 1997) which is about the ESR dating of tooth enamel from Yunxian *Homo Erectus* site, China. In this paper we report our ESR dating work on nine tooth enamel samples excavated from a very important *Homo Erectus* site in Yunxian County, China, which are stratigraphically associated with two almost complete fossil hominid crania. The ESR ages we achieved have an average of 581 ± 93 kyr. Interestingly, this age is again younger than the age previously assigned by the method of geomagnetic dating, which resulted in 830-870 kyr. Nonetheless, the ESR dating results "place the Yunxian crania in between the *Homo Erectus* of Lantian and Zhoukoudian which indicates that Yunxian crania constitute an important link in the human evolutionary lineage of China."(Chen, et al., 1997)

Besides the detailed investigation of other aspects in ESR dating, we again used the computer programme DATA to calculate the ESR ages. The results are, inevitably, younger than the revised ages by ROSY programme, as shown in Table 4.4. However, this time, the difference is very small, and only 3.1 % of average difference is observed between the DATA calculated ESR ages and ROSY calculated ages. This is reasonable, because as will be shown in Table 4.5, the details of the nine samples indicate that the uranium concentration in both tooth enamel and dentine are very high, while high tooth enamel uranium concentration means high internal alpha and beta doses and lower proportion of external beta dose, thus the difference between the DATA calculation and ROSY calculation should be small, moreover, the tooth enamel samples we prepared in this site are all from the

outside of the teeth, and the external beta dose from sediment is minor due to its lower radioisotope concentrations.

There are numerous examples to illustrate the impact induced by the new age calculation programme ROSY, and generally, the revision will lead to older ESR ages than the existing ones. The difference is anticipated to be from 0% (e.g. sample 5 in Table 4.2) to 30% (e.g. sample 1 in Table 4.2) according to individual cases, and the influence of these changes will be significant. In short, our experimental results will become a challenge to the field of ESR dating, especially to the existing ESR ages.

Table 4.4 Comparison of ESR ages calculated by ROSY and DATA (Yunxian Site, China)

Sample numbers	DATA calculated ages (ka)	ROSY calculated ages (ka)
y92002	588 ± 144	628 ± 153
y92006	687 ± 110	702 ± 115
y92008	477 ± 73	489 ± 74
y92009	686 ± 156	720 ± 151
y93101	455 ± 57	457 ± 58
y93102	572 ± 190	574 ± 183
y93103	517 ± 81	519 ± 67
y93104	541 ± 126	562 ± 131
y92011	704 ± 124	737 ± 130
Average ESR ages	**581 ± 93**	**599 ± 118**

The difference between the DATA calculated ages and ROSY calculated ages ranges from almost zero (samples y93101, y93102) to 6.8% (sample y92002).

Table 4.5 Original data for age calculation (Yunxian Site, China)

Sample	AD (Gy)	Enamel U(ppm)	Enamel $^{230}Th/^{234}U$	Enamel $^{234}U/^{238}U$	Dentine U(ppm)	Dentine $^{230}Th/^{234}U$	Dentine $^{234}U/^{238}U$	EU age (ka) (by DATA)	LU age (ka) (by DATA)
y92002	5636±1170	16.1±2.0			84.0±3.0			588 ± 144	1050 ± 251
y92006	5464±600	14.4±0.6	1.068±.051	1.35±.06	36.3±2.0			687 ± 110	1213 ± 183
y92008	7343±700	30.9±2.0			89.7±3.8	1.255±.057	1.573±.055	477 ± 73	899 ± 131
y92009	7726±1500	19.8±2.0			85.9±4.6	1.174±.066	1.555±.059	686 ± 150	1252 ± 277
y93101	5806±300	27.6±0.9	1.084±.044	1.24±.04	31.8±2.0			455 ± 58	834 ± 101
y93102	6615±2000	22.5±1.5	1.066±.069	1.45±.08	24.1±2.0			572 ± 190	1047 ± 342
y93103	4788±400	19.0±1.0	1.068±.042	1.23±.04	24.1±2.0			516 ± 81	921 ± 137
y93104	5755±1000	19.8±2.0			81.5±3.0			541 ± 126	982 ± 214
y92011	6745±900	17.3±0.6	1.075±.049	1.22±.04	76.9±3.2	1.260±.062	1.132±.056	704 ±125	1261 ± 214
Mean ± STD								581 ± 93	1051 ± 150

The annual dose rates were calculated on the base of the uranium contents of both enamel and dentine, or in case of surface enamel layer, the U, Th and K contents of the surrounding soil were also taken into consideration. The uranium concentration in the soil is measured to be (1.9 ± 0.2) ppm, the thorium concentration is (7.1 ± 1.0) ppm, and potassium is (1.5 ± 0.2) %, for all nine samples.

CHAPTER 5

CONCLUSIONS AND FINAL REMARKS

Electron spin resonance (ESR) dating is a very promising method in geochronology, because it covers the dating range from several thousand years to several million years, and can be applied to dating in sites that lack materials needed for conventional approaches. This technology is still under revisions but its usage is extending. (Rink, 1997& Schwarcz, 1994)

Based on the research work we have done regarding the beta attenuation problem, which is described in this thesis, we believe that the method of beta dose calculation in the ESR dating software DATA is problematic. Our experimental results firmly support the prediction of ROSY programme on the issue of beta dose attenuation under planar geometry, which is the major difference between the two computer programmes DATA and ROSY, and thus raises the question if we have enough confidence to revise all the ESR ages previously calculated using DATA by the computation of ROSY programme. Examples were chosen to see how much difference the revision could make, and showed that ages can change by up to 30%. In the case of Jinnuishan, we found out that the revised ages were more acceptable than the old DATA calculated ages, which strengthened our confidence in our results. The experimental confirmation of "one group" theory is a key finding that

requires the first major revision of ESR tooth enamel ages. We also note that it may also strongly affect ESR ages on mollusc shell calculations with DATA.

Of course, our confidence is also built-up on the correctness of our theoretical basis to calculate the beta dose, which is the "one group" transport theory. Most recently, a paper published by Prestwich et al. (1997) literally explained the concept of "one group" transport theory and also provided very straightforward experimental results to support their estimation using "one group" theory in beta dosimetry. Their results actually support our argument in ESR dating. Another very important theoretical and experimental evidence to support the "one group" theory is from the work done by O'Brien et al (1964), in which they compared their theoretical predictions of beta dose attenuation using "one group" theory with their experimental results achieved by a sophisticated experimental arrangement. Their experimental data points fitted in exactly the theoretical predictions. Moreover, the theoretical predictions by "one group" transport theory have fairly good agreement with the results of Monte Carlo simulation, which is considered to be the best approach in the radiation dosimetry. So, with all these evidences, I think it's not too unreasonable to draw the conclusion that the "one group" transport theory is more reliable than the approximation of Yokoyama (1982) which is employed by R. Grün (1986) in the DATA programme.

REFERENCE

Aitken, M.J. (1985). ***Thermoluminescence dating***. Academic Press, London.

Aitken, M.J., Clark, P.A., Gaffney, C.F. & Lovborg, L. (1985). Beta and gamma gradients. ***Nucl. Tracks***, vol.10, pp.647-653.

Brennan, B.J., Rink, W.J., McGuirl, E.L., Schwarcz, H.P. & Prestwich, W.V. (1997). Beta doses in tooth enamel by "one group" theory and the ROSY ESR dating software. ***Radiation Meas.***, vol.27, pp.307-314.

Chen, T.M., Yang, Q. & Wu, E. (1994). Antiquity of *Homo sapiens* in China. ***Nature***, vol.368, pp.55-56.

Chen, T.M., Yang, Q., Hu, Y.Q., Bao, W.B. & Li, T.Y. (1997). ESR dating of tooth enamel from Yunxian Homo Erectus site, China. ***Quat. Sci. Rev. (Quat. Geochron.)***, vol.16, pp.445-458.

Chen, T.M. & Yuan, S.X. (1988). Uranium-series dating of bones and teeth from Chinese palaeolithic sites. ***Archaeometry***, vol.30, pp.59-76.

Cross, W.G., Ing. H. & Freedman, N. (1983). A short atlas of beta ray spectra. ***Phys. Med. Biol.***, vol.18, pp.1251-1260.

Evans, R.D. (1955). ***The Atomic nucleus***. McGraw-Hill Book Company, INC.

Flammersfeld, A. (1946). ***Naturw.***, vol.33, pp.280-281.

Grun, R. (1986). Beta dose attenuation in thin layers. ***Ancient TL***, vol.4, pp.1-8.

Grun, R. (1989). Electron spin resonance (ESR) dating. ***Quaternary international***, vol.1 pp. 65-109.

Ikeya, M. (1993). ***New application of electron spin resonance (dating, dosimetry and microscopy)***. World Scientific.

Kase, K.R., Bjarngard, B.E., Attix, F.H. (1990). ***The dosimetry of ionization radiation*** (volumes I, II, III). Academic Press, INC.

Lewis, H.W. (1950). Multiple scattering in an infinite medium. ***Phys. Rev.*** vol.78, pp.526

Mejdahl, H. (1979). Thermoluminescence dating: beta dose attenuation in quartz grains. ***Archaeometry***, vol.21, pp.61-72.

Miles, A.E.W. (1967). ***Structural and chemical organization of teeth (II)***. Academic Press.

Miles, A.E.W. (1972). ***Teeth and their origins***. Oxford University Press.

Nambi, K.S.V. & Aitken, M.J. (1986). Annual dose conversion factors for TL and ESR dating. ***Archaeometry***, vol.28, pp.202-205

O'Brien, K., Samson, A., Sanna, R. & McLaughlin, J.E. (1964). The application of "one group" transport theory to beta-ray dosimetry. ***Nucl. Sci. and Eng.***, vol.18, pp90-96.

Prestwich, W.V., Nunes, J.C. & Kwok, C.S. (1997). Beta interface dosimetry in the "one group approximation". ***Radiat. Phys. Chem.*** vol.49, No.5, pp.509-513

Rink, W.J., Schwarcz, H.P., Lee, H.K., Cabrera Valdes, V., Bernaldo de Quiros, F. & Hoyos, M. (1996) ESR dating of tooth enamel: comparison with AMS ^{14}C dates at El Castillo Cave, Spain. ***J. of Archaeol. Sci.***, vol.23, pp.945-951.

Rink, W.J. & Schwarcz, H.P. (1995). Tests for diagenesis in tooth enamel: ESR dating signals and carbonate contents. ***J. Archaeol. Sci.***, vol.22, pp.251-255.

Rink, W.J. (1997). Electron spin resonance (ESR) dating. (ESR applications in Quaternary Sciences and Archaeometry). ***Radiation Measurements.*** (in press)

Schwarcz, H.P. (1994). Current challenges to ESR dating. ***Quat. Sci. Rev. (Geochron.)*** vol.13, pp.601-605

Yamashita, T., Ohnishi, H., Yasuno, Y. (1972). Thermoluminescent dosimeter (TLD) II, Construction and characteristics of $CaSO_4$:Tm TLD. ***Technical Report***, vol.18, No.2 (Matsushita Electric Industrial CO., LTD.).

Yokoyama, Y., Nguyen, H.V., Quaegebeur, J.P. & Poupeau, G. (1982). Some problems encountered in the evaluation of annual dose rate in the electron spin resonance dating of fossil bones. ***PACT*** vol.6, pp.103-115